

A perspective on the pathway to a scalable quantum internet using rare-earth ions

Robert M. Pettit¹, Farhang Hadad Farshi², Sean E. Sullivan¹, Álvaro Véliz-Osorio², and Manish Kumar Singh¹

¹memQ Inc., 5235 S. Harper Ct. 8th Floor, Chicago, IL, 60615, USA

²Da Vinci Labs, 2 côte de la Guêpière, 37530 Nazelles-Négron, France

The ultimate realization of a global quantum internet will require advances in scalable technologies capable of generating, storing, and manipulating quantum information. The essential devices that will perform these tasks in a quantum network are quantum repeaters, which will enable the long-range distribution of entanglement between distant network nodes. In this perspective, we provide an overview of the primary functions of a quantum repeater and discuss progress that has been made toward the development of repeaters with rare-earth ion doped materials while noting challenges that are being faced as the technologies mature. We give particular attention to erbium, which is well suited for networking applications. Finally, we provide a discussion of near-term benchmarks that can further guide rare-earth ion platforms for impact in near-term quantum networks.

1 Introduction

The quantum internet promises to revolutionize computing, communication, and sensing [1–3]. The processing power offered by *networked* quantum computers could be scaled beyond what is possible with a single quantum computer, finding useful applications in problems of materials science, pharmaceuticals, and optimization among others that classical computers would find intractable. Additionally, a quantum internet would allow communication between users where the security of transmitted data can be guaranteed by the laws of quantum physics [4]. This connectivity could also be exploited to link up measurement devices such as atomic clocks [5] or telescopes [6] to advance the state-of-the-art in timekeeping and astronomy, as well as to test the fundamentals of quantum mechanics across unprecedented length scales [7].

A quantum internet will consist of nodes of quantum processors and channels to distribute entanglement between the nodes. Each channel will therefore be required to preserve fragile quantum entanglement. This demand is a steep challenge to meet. The ultimate size of a quantum internet will depend on how well the channels are able to fulfill this task.

An optical photon is the ideal mediator of entanglement throughout the network due to its ability to propagate through existing low-loss networks of optical telecommunications

Robert M. Pettit: robert.pettit@memq.tech

Manish Kumar Singh: manish@memq.tech



Figure 1: An urban-scale quantum network in Chicago, IL, USA. The network nodes span 200 km of optical fiber. Image courtesy of the Chicago Quantum Exchange.

fiber. Photons may also be beamed across free-space links [8] or to satellites from ground-based nodes [9]. In this review, we focus on fiber network applications with the view that, in the near-term, optical fiber connections will be used to span local networks with links over 100s of km, while satellites may be reserved to connect more distant nodes separated by 1000s of km or more [10, 11]. Construction of urban-scale fiber networks for quantum networking is ongoing in various metropolitan areas around the world to establish test beds for exploring quantum communications technologies under real world operating conditions [11–16]. These networks may then provide the necessary initial infrastructure for building out larger networks to develop a global scale quantum internet. As an example, figure 1 shows an urban-scale network constructed across the Chicago, IL, USA metro area that connects nodes across 200 km of optical fiber.

Even in state-of-the art low-loss fiber, photon losses scale exponentially at rates of about 0.2 dB/km. For wavelengths outside of the telecom window, the loss rates are higher. In classical telecommunications networks, repeaters are used to boost the signal to overcome this inherent loss in the fibers. A full-scale quantum internet will therefore need nodes that can connect via optical fiber, as well as repeaters that can assist with distributing entanglement between the nodes by fighting losses present in the fiber channels. These quantum repeaters will be fundamentally different from repeaters in classical telecommunications networks, however, because the no-cloning theorem prevents the amplification of arbitrary quantum states [17]. Quantum repeaters will have three main essential capabilities: (i) the ability to produce entanglement between stationary matter qubits and photonic “flying” qubits, (ii) the ability to store arbitrary quantum states in memory for asynchronous entanglement creation between distant nodes, and (iii) the ability to perform entanglement swapping operations to distribute entanglement across the network.

On a physical level, an ideal quantum repeater would deliver on-demand single or entangled photons at a high rate for fast data transfer, operate at telecom wavelengths for long-distance transmission over optical fiber, and exhibit long optical or spin coherence times to enable entanglement operations over timescales commensurate with the time-of-flight of photons across the optical channels. A variety of modalities are under development to enable a quantum internet via optical channels, in particular modalities that utilize atom-like emitters in the solid-state [18, 19]. A major challenge is that all of these

modalities face a trade off between the photon emission wavelength, photon emission rate, and the photon or spin coherence times that ultimately limit the suitability of the modality for realizing a quantum repeater. While some modalities, such as semiconductor quantum dots or vacancy complexes in materials such as diamond and SiC, meet one or two of these criteria, few can meet all three without additional engineering. Rare-earth ions embedded in a solid-state host have demonstrated emission at telecom wavelengths as well as long optical and spin coherence times, however they do not inherently deliver photons at a fast rate. The limited photon emission rate can be overcome by engineering on-chip cavities and waveguides to achieve Purcell enhancement [20] and efficient routing of the emission. The combination of rare-earth ions embedded in solid-state hosts with engineered nanophotonic devices can therefore achieve all three necessary criteria to develop quantum repeaters.

Toward this goal, advances in engineering with rare-earth ion platforms have also demonstrated the critical ability to integrate with scalable photonics platforms, either in silicon [21–25], lithium niobate [26–30], silicon nitride [31–33] or doped thin films grown on silicon [34, 35]. Compatibility with standard semiconductor foundry processes is an essential feature for any modality that will be able to scale to the necessary size to enable a quantum internet. For example, it is expected that individual repeater nodes will need on the order of hundreds or thousands of physical qubits for fault-tolerant operation depending on the system metrics and protocols used [36–38]. This illustrates the size of the challenge to develop a quantum internet that will require extensive networks of repeaters and underscores the need for scalable and repeatable fabrication processes.

In this review, we discuss the potential for rare-earth ions embedded in a solid-state host to enable a quantum internet through the development of quantum repeaters. We first outline the essential elements of a quantum network, including protocols for the generation, storage, and distribution of entanglement. We then discuss the properties of embedded rare-earth ions in the context of the needs of a quantum network and provide an overview of state-of-the-art developments and outstanding challenges that pertain to the development of repeaters with embedded rare-earth ions. We give particular consideration to erbium, which in its Er^{3+} state is particularly suitable for quantum networking applications and we indicate some near term benchmarks that can be realized by scalable devices for impact in developing quantum networks. Finally, we provide a perspective on how rare-earth ion technologies may further enable the growth of future quantum networks by connecting different qubit modalities using quantum state transduction protocols. These protocols have the power to connect otherwise disparate qubit modalities and will be a boon for the development of global and multi-functional quantum networks.

2 Quantum networks

The essential function of a quantum network is to distribute information processing efficiently across a web of local quantum computing machines, sensors, and communication devices that are easily controllable, as shown in figure 2. The possibility of such a construct however, seems to be determined by a number of conditions that do not appear to be readily compatible with each other if physically realized. Local processing units or nodes are systems where information is processed and stored for long time. Such systems are required to be implemented using quantum hardware that on the one hand exhibit a prolonged coherence time by being well isolated from the surrounding environment, and on the other hand, are highly amenable to controlled interactions with ancillary systems. Moreover, the communication of quantum data across various nodes can only be realized using systems that can traverse long distances with negligible decoherence such as optical

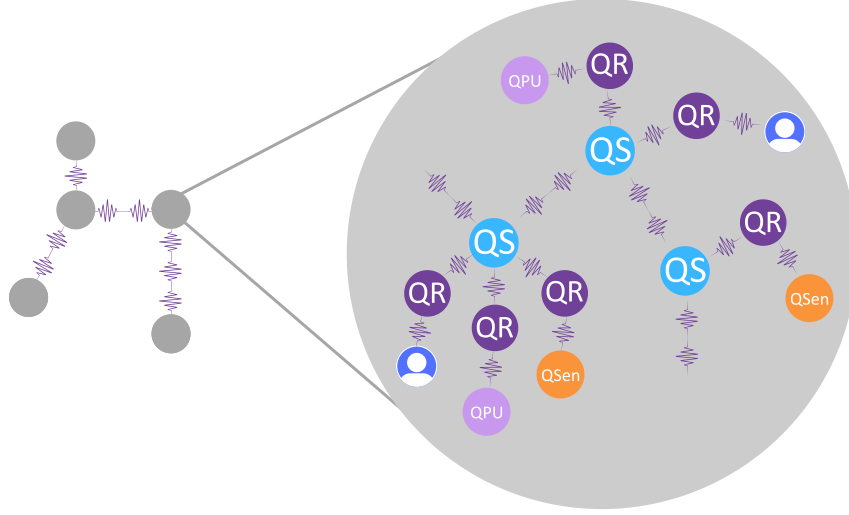


Figure 2: A quantum network where nodes are interconnected via photonic channels. The network comprises multiple length scales where quantum repeaters (QR) and quantum switches (QS) facilitate the distribution of entanglement across local and distant nodes for secure communication between users, quantum processors and computers (QPU), and measurement devices and sensors (QSen).

photons. Having such weakly-coupling particles interacting with nodes in a controlled way as to mediate information between them seems to be another challenge in building a functional quantum network. Therefore, it seems that the possibility of a quantum network hinges on the ability to realize highly controlled interactions between well isolated nodes such as trapped atomic systems and photons forming a hybrid system of light and matter.

Quantum networks, depending on their task, can be divided into two main categories: computation networks and communication networks. The function of a quantum computation network is to spread entangled states across a large number of nodes that are interconnected by photons to perform large-scale information processing tasks. A modular distributed quantum computer [39, 40] where nodes (logical processing units) are linked through a photonic network is paradigmatic of a quantum computation network, which is capable of supporting universal one-way quantum computation [41]. A communication network on the other hand is a scheme to generate a maximally entangled state shared over arbitrary large distances. In what follows, we will have a quick look at the blueprint of a quantum network within the two aforementioned paradigms.

Modular quantum computation; A modular architecture consists of a collection of nodes that are linked through photonic interfaces. Each node is a sequence of qubits that are amenable to fast and deterministic local interactions for realizing single and two-qubit logic gates with error rates sufficiently low to perform fault-tolerant computation. Within each node, the qubits are divided into two classes: memory qubits on which information is processed and stored, and communication qubits that are linked to their counterparts situated within another node through a photonic channel. The function of communication qubits is to facilitate the implementation of two-qubits gates between any pair of memory qubits, one from each node by means of indirect interaction mediated by photons. This architecture allows for the construction of cluster states shared among a large number of nodes offering a platform to run measurement-based fault-tolerant universal quantum computation [42].

Quantum communication; A quantum communication network is an alternative architecture that can essentially be thought of as a modular quantum computer with a linear

topology. The function of a quantum communication network is the distribution of purified maximally entangled states shared exclusively between a pair of nodes separated by an arbitrary large distance. This can be achieved either by constructing a cluster state across the network and performing local gates on intermediary nodes as to distill a maximally bipartite entangled state shared between the end-nodes, or alternatively, by means of entanglement swapping between neighboring nodes in a successive hierarchical fashion [43].

Central to the functioning of quantum networks discussed above is the capacity to implement what is referred to as *quantum repeater scheme* [43]: a protocol that can *generate*, *store* and *distribute* entanglement amongst pairs of spatially separated quantum nodes *efficiently*. That is, the key to a realistic quantum network is the ability to perform the following three steps with arbitrary degree of accuracy, and with a polynomial overhead in the resources: (i) generating entanglement between the communication qubits mediated by photons, (ii) transferring the induced entangled state onto the memory qubits for storage, and (iii) connecting and purifying the stored entangled states across the network through local operations. In what follows, we provide a minimal review on the schemes that realize these three steps.

2.1 Entanglement generation

The core algorithm underlying the generation of entanglement between a pair of nodes is illustrated in figure 3: first an entangled qubit-photon pair is generated within each node, and then a Bell-state measurement of the collected photons projects the nodes onto an entangled state. We will briefly summarize the two main protocols that realize this entangling circuit.

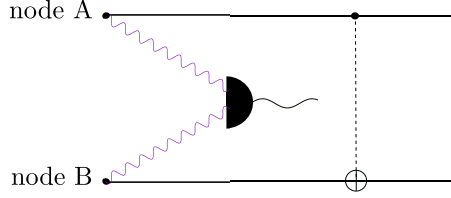


Figure 3: At each node a qubit-photon pair is generated. Photons are collected for a Bell-state measurement. Detection of a single photon would herald the generation of an entangled state shared between the nodes.

2.1.1 Single emitters

In this approach [44, 45], each node consists of an atomic system with an effective three-level Lambda configuration - which comprises two relatively stable low lying states $\{|\uparrow\rangle, |\downarrow\rangle\}$ encoding the qubit state, and an excited state $|e\rangle$ - situated within an optical cavity, which is schematically depicted in figure 4. Both of the qubit systems are initially prepared in a superposition state forming the product state $[\frac{1}{\sqrt{2}}(|\uparrow\rangle + |\downarrow\rangle)]^{\otimes 2}$. Next, each qubit is driven by a control pulse that is resonant with the $|\downarrow\rangle \rightarrow |e\rangle$ transition. From this moment on, the effective dynamics of the system is governed by the Jayne-Cummings Hamiltonian:

$$H = \sum_{i=1}^2 g_i (\sigma_i^- a_i^\dagger + \sigma_i^+ a_i), \quad (1)$$

where g_i denotes the coupling between the qubit and the cavity mode, and the σ_i^\pm ($\{a, a^\dagger\}$) correspond to the creation and annihilation operators associated with the qubit (cavity

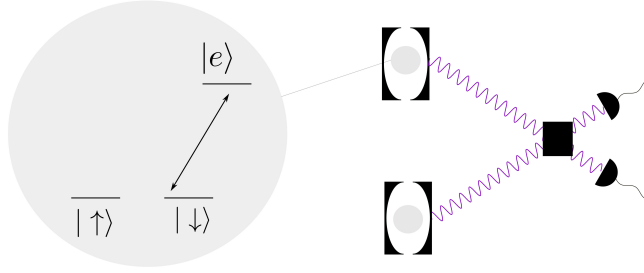


Figure 4: In each cavity a three-level system (a qubit system $\{|\uparrow\rangle, |\downarrow\rangle\}$ plus an excited state $|e\rangle$) is situated. Driving the $|\downarrow\rangle \rightarrow |e\rangle$ transition, followed by the emission of a photon brings the excited state back to $|\downarrow\rangle$. Conditioned on the observation of a single photon at the detection outputs, the entire state is projected onto an entangled qubit state.

photon). As the Hamiltonian 1 indicates, the transition $|\downarrow\rangle \leftrightarrow |e\rangle$ is coupled to the cavity mode, which after a short period of time causes the qubit to undergo a spontaneous emission that results in a locally entangled state shared by the qubit and the emitted photon in the cavity resulting in the state $|\psi\rangle = [\frac{1}{\sqrt{2}}(|\downarrow 1\rangle + |\uparrow 0\rangle)]^{\otimes 2}$. The emitted photons are then collected from the cavities and are guided towards a beam splitter just before being measured in an optical detection output. The function of the beam splitter is to erase the information regarding the trajectory that each photon has taken, so that the detection of a single photon could have originated from either of the nodes. In this way, conditioned on the observation of a single photon, the collective state of the qubit-photon pair is updated under the action of the emission operator $l_{\pm} = \frac{1}{\sqrt{2}}(a_1 \pm a_2)$:

$$l_{\pm}|\psi\rangle \rightarrow |\phi_{\pm}\rangle + |\zeta_{\pm}\rangle, \quad (2)$$

where $|\phi_{\pm}\rangle \propto (|\uparrow\downarrow\rangle \pm |\downarrow\uparrow\rangle)|00\rangle$ denotes the desired maximally entangled state between the qubit pair, and $|\zeta_{\pm}\rangle \propto (|01\rangle \pm |10\rangle)|\downarrow\downarrow\rangle$. As the equation 2 indicates, there exists the possibility of a second photon being observed, which is encoded in $|\zeta_{\pm}\rangle$. However, due to experimental imperfections such as photon loss and limited efficiency of the detectors, the state $|\zeta_{\pm}\rangle$ is, as well, compatible with the single photon detection with a non-vanishing probability. That is, the residual entanglement between the qubit-pair and the photon-pair can not be removed due to imperfect knowledge of the system, which leads to the decoherence of the qubit-pair into a mixed state

$$\rho = p_1|u_1^{\pm}\rangle\langle u_1^{\pm}| + p_2|u_2\rangle\langle u_2| \quad (3)$$

where $|u_1^{\pm}\rangle = \frac{1}{\sqrt{2}}(|\uparrow\downarrow\rangle \pm |\downarrow\uparrow\rangle)$, and $|u_2\rangle = |\downarrow\downarrow\rangle$. The way to suppress the second term in the equation 3 is to flip the qubit states, $|\downarrow\rangle \leftrightarrow |\uparrow\rangle$ and repeat the previous procedure. In this way, the state $|\downarrow\downarrow\rangle$ is turned to $|\uparrow\uparrow\rangle$, which cannot contribute to any emission, whereas the state $|u_1^{\pm}\rangle$ would still emit a single photon. Therefore, the observation of a single photon per each cycle would herald the generation of a pure entangled state $|u_1^{\pm}\rangle$ among the qubit-pair.

The fidelity of this entangling protocol can be affected by various sources of error, of which two main categories are the decoherence of the qubit systems and the reduced indistinguishability of the photon pairs [46]. Decoherence of the qubit due to its unavoidable coupling to the environment leads to the reduction in the initial entanglement measure between the qubit and the photon, which has a direct detrimental impact on the amount of

the ultimate entanglement induced between the qubit-pair. The distinguishability between the photons is another source of infidelity as the functioning of the protocol hinges on the inability of the measuring apparatus to discern from which node the photon arrives. This condition requires accurate control over the qubit-photon interaction, photon emission, frequency and polarization.

2.1.2 Atomic ensembles

One of the key requirements for single emitters to function as communication qubits is having them situated within optical resonators of very high quality. An alternative approach that bypasses this challenge is to use an ensemble of single emitters, which greatly enhances the control over photon generation due to their collective effect. A remarkable entangling scheme that is based on the atomic ensemble, and which we refer to as the DLCZ protocol [47] involves a pair of ensembles each described effectively as a collection of three-level Lambda systems with two ground state $\{|\uparrow\rangle, |\downarrow\rangle\}$, and an excited state $|e\rangle$. Each ensemble is prepared at the ground state before being driven by a radiation pulse that is off-resonant on the transition $|\downarrow\rangle \leftrightarrow |e\rangle$, which leads to a spontaneous Raman emission $|e\rangle \leftrightarrow |\uparrow\rangle$. This leads to the generation of a Stokes photon and a single atomic excitation (logical state $|\uparrow\rangle$) smeared over the entire ensemble:

$$|\uparrow\rangle = \frac{1}{\sqrt{N}} \sum_{i=1}^N \alpha_i |\downarrow\rangle_1 |\downarrow\rangle_2 \dots |\uparrow\rangle_i \dots |\downarrow\rangle_N \quad (4)$$

where the phase factor α_i depends on the radiation mode and the position of the i th atom, and N denotes the total number of the atoms within the ensemble. The interaction between the emitted photon and the ensemble described above is effectively captured by the Hamiltonian:

$$H = g(s^\dagger a^\dagger + sa) \quad (5)$$

where g denotes the coupling constant that is a function of the pulse intensity, number of atoms within the ensemble and the strength of the Raman transition, and a and s denote the annihilation operator for Stokes photon and the atomic excitation respectively. The evolution induced by this Hamiltonian generates an ensemble-photon pair entangled state that can be written as a series expansion for small values of gt :

$$e^{-iHt} |\downarrow\rangle|0\rangle \rightarrow |\downarrow\rangle|0\rangle + ip^{\frac{1}{2}} |\uparrow\rangle|1\rangle + O(p) \quad (6)$$

where $p = (gt)^2$ denotes the probability for a single Stokes photon emission. At this stage, in a similar fashion to the single-emitter scheme discussed above, the Stokes photons are collected from both of the ensembles, and sent into a beam-splitter as to erase the which-way information of the photons before being observed at the detection outputs. Conditioned on a single photon being detected, the state of the entire system is updated under the spontaneous emission operator $l_\pm = \frac{1}{\sqrt{2}}(a_1 \pm a_2)$ that induces the desired entangled state shared between the ensemble pair:

$$l_\pm (|\downarrow\rangle|0\rangle + ip^{\frac{1}{2}} |\uparrow\rangle|1\rangle)^{\otimes 2} \rightarrow p^{\frac{1}{2}} (|\downarrow\uparrow\rangle + i|\uparrow\downarrow\rangle)|00\rangle + O(p). \quad (7)$$

As equation 7 indicates, the generated entangled state is not pure due to the presence of multi-photon emission with the probability $O(p)$. In order to suppress these higher order terms one needs to work with very low emission rate p , which in return, reduces

the probability for generating the entangled state itself, and subsequently, prolonging the protocol duration. Therefore, to be able to distribute the prepared entangled state across a network via the swapping operation, it is necessary for the ensemble-pair system to have a long coherence time for being able to store the heralded entanglement while the adjacent pair is undergoing the protocol.

2.2 Entanglement storage

Once the generation of entanglement between a pair of nodes is heralded, the next step is to map the shared state onto a quantum memory for storage and processing. Depending on the function that a quantum network performs the state mapping process can be divided into two separate classes: (1) for a quantum computation network where each node consists of a sequence of single emitters, the state is transferred from a communication qubit onto a memory qubit with long coherence through controlled local unitary gates at each node; (2) for a quantum communication network however, the atomic ensembles function both as communication and memory qubit and therefore the state-mapping procedure is no longer needed.

As we discussed earlier single emitters are a prime candidate for realizing distributed quantum information processing due to their high degree of controllability both in terms of their coupling to photonic channels, and their interaction with neighboring counterparts for unitary logic operations. One of the challenges linked with single-emitter-based architecture however, is to eliminate cross-talk between the interactions that a communication qubit undergoes with the photonic interface and with the memory qubits [40]. This means that a communication qubit must be well isolated from the rest of the node in order to prevent the unwanted excitation of the memory qubits, since such excitation caused by the scattered photons can introduce irreversible error channels in the computational tasks running within the node. There are two ways to effectively shield the memory qubits from the scattered photons. One way is to spatially separate the communication qubit from the rest of the node during the photon exchange. In this scheme, the communication qubit is physically transported to an optical cavity situated at a safe distance from the memory qubits for entanglement operation. Once the entanglement is established, the communication qubit is brought back to the vicinity of the other qubits for the state transfer operation via local unitary gates. Despite the effective isolation that such scheme offers, it requires a highly precise manipulation of the communication qubit during the transport, which leads to an increase in the control overhead. An alternative way to suppress such cross-talks is to utilize different atomic species with distinct transition frequencies for communication and memory qubits. In this way the photon emitted from a communication qubit would simply be invisible to the rest of the node as its frequency is sufficiently off with respect to the memory qubits' resonance frequency. Moreover, the division of each node into different atomic species allows for more flexibility in the choice of qubits since unlike the memory qubits, it is not necessary for the communication qubits to have long coherence characteristic, for once the entanglement between them is induced their state can be promptly written onto the memory qubits.

The alternative design for quantum nodes in a communication network involves atomic ensembles [48, 49] which as we discussed above exhibit deterministic interactions with photons without utilizing any cavity enhancement techniques thanks to their collective effect. A salient aspect of atomic-ensemble-based quantum memories is their multi-modal storage capacity [50]. In the entanglement creation protocols discussed above, the heralding of the established entanglement entails the emitted photon traveling to the measurement output and the result of a positive detection traveling back to the node. In this way, the

overall rate at which such protocol can be repeated is bounded by the communication time $\tau \propto L/c$ where L denotes the photonic channel length. To overcome this limitation schemes that utilize multi-mode memory systems that can store large numbers of distinguishable photonic modes have been proposed [50–52]. More concretely, using quantum memories that can store N distinct modes would allow for the N -times repetition of the entangling protocol per communication time, which improves the entanglement generation rate by a factor of N , and therefore the requirement for a quantum memory to have extremely long coherence time can be relaxed by the same factor. Various types of degrees of freedom can be chosen as to form the basis for these modes such as spatial or spectral modes of the photons. A desirable option however, is to utilize the distinguishable temporal modes or the time-bin degrees of freedom linked with the photon, which is also naturally suited for the transmission of information used in current telecommunication networks. The main entangling scheme that is well adapted for temporal multiplexing is a variation of the DLCZ protocol where the entanglement generation and storage are separated. In this approach [51], photon pair sources and absorptive memories are integrated as to emulate a sequence of DLCZ operations per communication time as illustrated in figure 5.

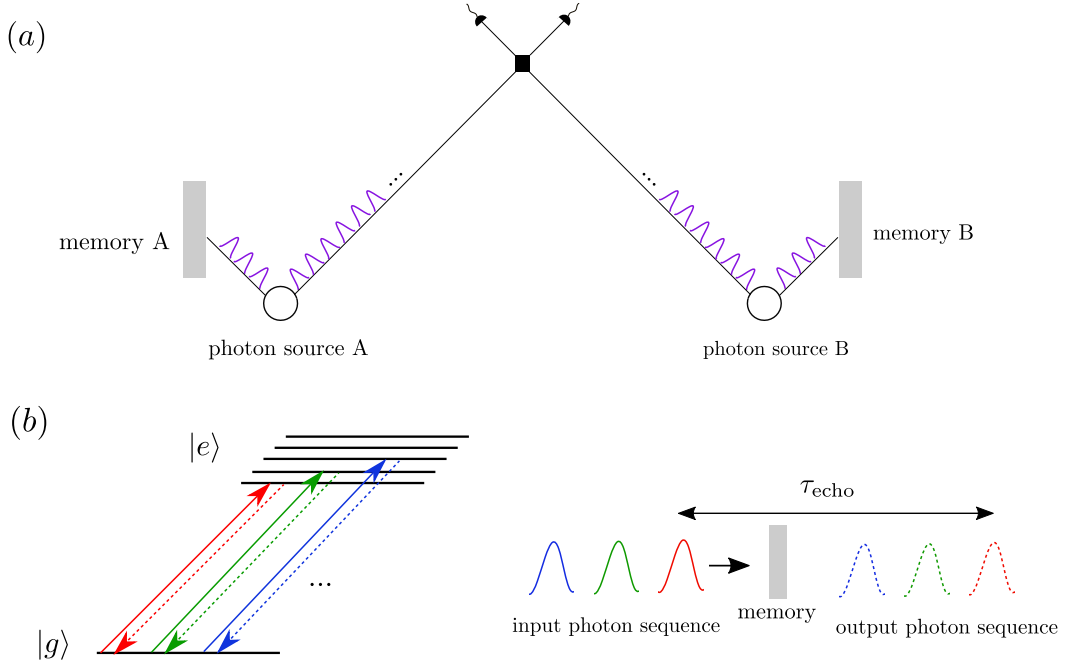


Figure 5: *a)* Entanglement generation scheme using temporal multi-mode memories: The photon sources at sites A and B where the memories are located can each emit an entangled photon pair into a sequence of distinct temporal modes where for each mode one is sent to the detection output and the other one is stored in the memory. The detection of a single photon behind the beam splitter would project the memories into an entangled state. The source can be triggered a large number of times in every communication time interval. *b)* Temporal multi-mode memory system based on photon echo principle: a sequence of photons are absorbed and re-emitted by a comb-structure profile that is induced through inhomogeneous broadening of the spectra linked with the atomic ensemble memory.

The entangling scheme summarized above is based on memory systems that offer storage in various distinguishable temporal modes $\{|0\rangle_i, |1\rangle_i\}$. There are varied methods to realize these temporal multi-mode memories, a class of which - referred to as photon echo principle - is well suited for atomic ensembles in solids such as crystals doped with rare-earth ions [53]. The essence of the techniques that are based on photon echo principle is to preserve the one-to-one temporal correspondence between the absorption and the emission

of each photon so that photons that are absorbed at separate moments are emitted at separate moments. The storage schemes that are based on echo techniques utilize reversible absorption of a single mode by a media the spectrum of which is subject to inhomogeneous broadening. Once the single photon is absorbed the memory state is mapped onto a collective atomic excitation :

$$|1\rangle = \sum_k c_k e^{i\delta_k t} |g_1\rangle |g_2\rangle \dots |e_k\rangle \dots |g_N\rangle \quad (8)$$

where δ_k denotes the detuning of the k th atom from the photon's central frequency. The core idea behind the echo technique is to steer the detuning spectrum such that after a certain period of time all the coefficients $e^{i\delta_k t}$ realign causing the memory state to re-phase. As a consequence the absorbed photon will be emitted in a well defined temporal mode thanks to the collective interference effect amongst all the emitters within the atomic ensemble. In this way the information regarding the temporal relation between a sequence of photons is encoded in the relative phases of the atomic excitations at different frequencies. As a result, a sequence of photons that are absorbed by the memory at different moments will be emitted at distinct instants of time each separated (from the absorption time) by a constant duration determined by the controlled re-phasing period.

2.3 Entanglement distribution

Once the entangled state is stored among pairs of nodes, the next step is to link these pairs as to share the entanglement between the nodes situated at large distances from each other that are not directly connected via photon channels. This can be done by performing an entanglement swapping operation [50] on the nearby nodes in a heralded fashion mapping the distant node-pair into an entangled state. The swapping operation consists of a Bell-state measurement on the intermediary nodes, and conditioned on the result the composite state of the end-point nodes is projected onto an entangled state. Let us imagine that two pairs of nodes $A - B$ and $C - D$ are each prepared in an entangled state given in (7). The information stored within the memories B and C is converted into photons propagating in well defined direction, and subsequently collected at a beam splitter as to erase their which-way information before being measured at detection outputs. Conditioned on the observation of a single photon the global state is updated under the emission operator $\frac{1}{\sqrt{2}}(a_B + a_C)$ projecting the memories A and D into an entangled state. The dominant source of error in a swapping operation is related to photon loss due to inefficiencies linked with detectors and memories. That is the measuring outputs can erroneously signal a single photon detection while having two photons stored in memories B and C , which leads to the presence of an additional vacuum component in the generated entangled state between A and D :

$$\rho_{AD} = p_1 |u_1^\pm\rangle \langle u_1^\pm| + p_2 |u_2\rangle \langle u_2| \quad (9)$$

where $|u_1^\pm\rangle = \frac{1}{\sqrt{2}}(|\uparrow\downarrow\rangle_{AD} \pm |\downarrow\uparrow\rangle_{AD})$, and $|u_2\rangle = |\downarrow\downarrow\rangle_{AD}$. In order to connect a pair of distant nodes separated by N links ($N - 1$ intermediary nodes) one needs to perform the swapping operation N times, and with each such connection the ratio p_1/p_2 decays. This leads to a rapid decrease in the fidelity of the induced entangled state shared between the end-point nodes such that at large N it will not be possible to error-correct the state using any purification protocol. To bypass this difficulty an error correction scheme called the nested purification protocol [43] has been proposed, which consists of connecting and purifying in a successive hierarchical fashion. The fundamental principle underlying this

protocol is the entanglement distillation that makes it possible to purify an entangled state to arbitrary degree of accuracy from an ensemble of noisy imperfect entangled pairs using only local operations at each node. The nested purification protocol can be carried out by iterating the following two steps: first applying the swapping operation to a small number of links $L \ll N$, producing an ensemble of noisy entangled pairs, and second performing local single and two-qubit gates on the connected nodes as to distill a smaller number of highly entangled states with suppressed error rates. It can be easily checked that if the number of elementary imperfect entangled states necessary to purify an state across L links is M , then the total number of such elementary states required for a network of $N = L^n$ links is $R = (LM)^n$. In other words, the overhead in the resources scales polynomially with N as R can be re-written as $R = N^{\log_L M + 1}$. M can be determined by a number of factors including the fidelity of the elementary imperfect raw entangled pairs, the network platform, the type of the distillation protocol used, and the nature of the dissipative processes involved in the operations of swapping and purification.

3 Rare-earth ion doped materials for quantum networking

The focus of this section is to describe the properties and capabilities of rare-earth ion doped materials in terms that are useful for constructing quantum communication networks as discussed in section 2. Rare-earth ions can interface with a range of optical wavelengths from the visible to the telecom, and also possess controllable and long lived spin states that make them compatible with many protocols and architectures for building out a quantum network. In this section, we aim to characterize these properties in terms of how they relate to the construction of quantum networks. We will focus on the ways rare-earth ion doped materials have been used for quantum resource generation, quantum resource storage, and quantum resource distribution. We will also outline some of the challenges that must be overcome for rare-earth ion doped materials to develop into a platform that can support large scale quantum networks.

Rare-earth elements are a grouping of metals in the periodic table that in their readily formed triply ionized state possess a partially filled $4f$ orbital shielded by filled $5s$ and $5p$ outer orbitals. The configuration of the unpaired electrons in the $4f$ orbital of Er^{3+} is illustrated in figure 6. The shielding of the $4f$ orbital allows the energy levels of the ion to experience only a slight and well understood perturbation when doped into a crystalline environment [54–56]. The unpaired electrons within the $4f$ orbital provide a variety of low lying spin levels that can be used as qubit states as well as excited electronic levels that can couple to optical photons. These properties underlie all the applications in quantum networking which are outlined in this section. An established understanding of the properties of both the ions and the chosen host crystals makes it possible to turn our attention to the goal of engineering devices that can then enable the development of quantum networks.

3.1 Quantum resource generation

3.1.1 Considerations for single photon sources

In the context of using rare-earth ions for quantum networking, we will consider quantum resource generation to refer to the production of single photons that can be used within a network. In accordance with the protocols outlined in section 2.1, these photons can then be used to generate or distribute entanglement throughout the network. The primary considerations for judging the quality of a single photon source as a resource for quantum

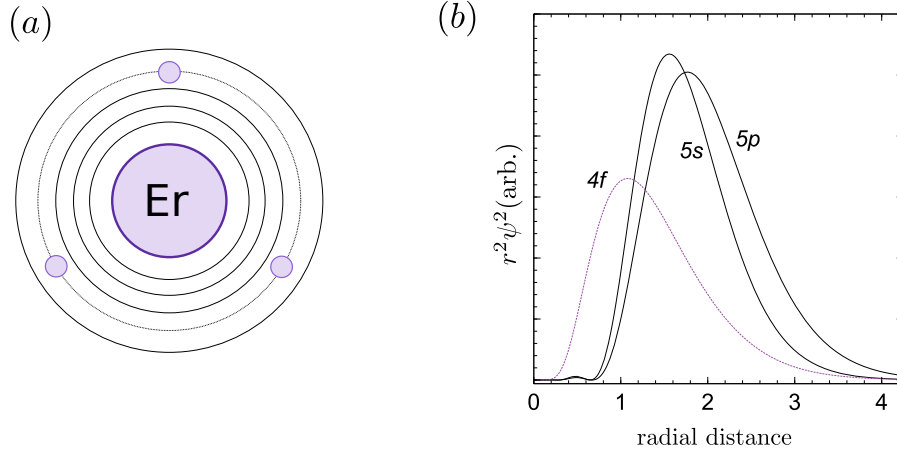


Figure 6: (a) Simplified picture of a rare-earth ion showing only the unpaired electrons orbiting the ion nucleus. Orbitals are drawn for the first five principle quantum numbers. Triply ionized erbium (Er^{3+}) is shown, having three unpaired electrons in the $4f$ orbital. (b) Radial wavefunctions for the outer orbitals of Er^{3+} as a function of distance from the nucleus. The unfilled $4f$ orbital is shielded by the filled $5s$ and $5p$ orbitals.

networking are the brightness, coherence time, and indistinguishability between the emitted single photons. Indistinguishability between photons is a measure that determines the degree to which the emitted photons are identical. It encompasses every property of a photon including wavelength and polarization, as well as spatial and temporal mode profile. The degree of indistinguishability between photons is the most important feature to consider for a single photon source to be used in a quantum network since photons must be indistinguishable to distribute entanglement, as highlighted in section 2. The source brightness determines how many single photons can be inserted into the network over a given time frame, and is closely related to the single photon emission probability which quantifies the errors that may occur due to undesired multi-photon emission events. In this regard, atomic and atom-like sources of single photons offer the advantage of near-deterministic operation [18, 57], while sources based on spontaneous parametric down conversion [58] or spontaneous four-wave mixing [59] rely on heralding to suppress multi-photon events. In general, sources with both a high brightness and a high single photon emission probability are required for different applications. Finally, the coherence time determines how long a photon can travel in the network and still interfere with another identical photon. In this section we outline how each of these properties are related to one another before discussing the progress that has been made so far in building single photon sources from rare-earth ions in solid-state media.

In the solid state, the properties of a single photon emitter are intimately related to the host material it is embedded in. A single photon source has an emission rate, γ , that is inversely related to the optical excited state lifetime of the emitter through the relationship $\gamma = 1/T_1$, where T_1 is the lifetime. Shorter excited state lifetimes therefore provide larger emission rates in the absence of non-radiative decay channels. If non-radiative decay channels exist, the total decay rate is the sum of the radiative and non-radiative parts, $\gamma = \gamma_r + \gamma_{nr}$, where γ_r and γ_{nr} are the radiative and non-radiative rates, respectively. An optically excited ion may then have a pathway to relax back to the ground state, or another state altogether, without emitting a photon in the desired mode. While these additional decay pathways may find use in control or read-out protocols [60], they are generally disadvantageous in applications that require the emission of single photons into a single

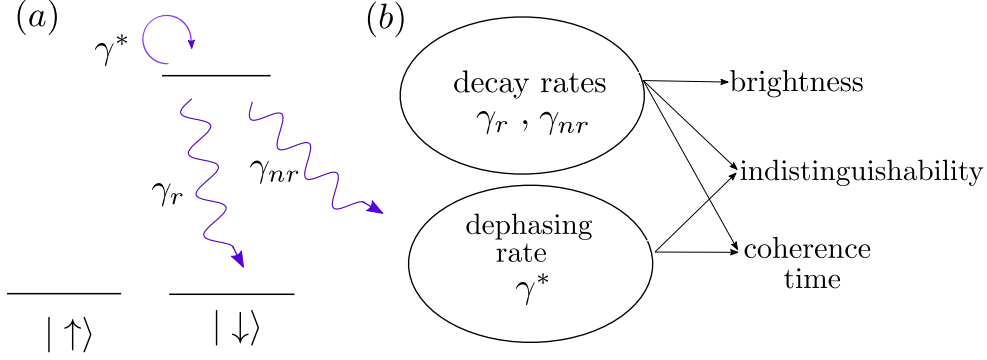


Figure 7: (a) A single photon emitting source subject to decay and dephasing mechanisms. (b) Outline of how decay and dephasing mechanisms are related to the brightness, indistinguishability, and coherence time of a single photon source.

optical mode. Therefore our goal is to limit the presence of non-radiative decay channels by choosing emitter and material combinations that minimize them [61]. We will also see in section 3.1.3 that there are other tools, in addition to emitter and host crystal choice, that allow us to improve the radiative properties single photon emitters. The brightness of the single photon source therefore depends critically on the radiative decay rate of the emitter, as well as how efficiently the emitted photons can then be coupled to the network. In order to achieve a high single photon emission probability, multi-photon emission can be suppressed by tailoring the excitation pulse duration to be sufficiently short with respect to T_1 to avoid re-excitation of the emitter [62].

When a photon is emitted, the coherence time of the photon is given by the Fourier transform limited value $T_2 = 2T_1$ if no additional dephasing mechanisms are present. Therefore an unavoidable trade-off between emission rate and coherence time exists. This trade-off must be considered when choosing a single photon source for a network, as the coherence time of the source can also effect the achievable spacing of the network nodes. Additionally, the host material may introduce optical dephasing mechanisms from interactions with phonons or fluctuating electric and magnetic fields [63]. These mechanisms can be incorporated into a dephasing rate, $\gamma^*/2 = 1/T_2^*$, where each dephasing mechanism has its own characteristic timescale, T_2^* . In the presence of this additional dephasing, the coherence time of the emitted photons becomes

$$\frac{1}{T_2} = \frac{1}{2T_1} + \frac{1}{T_2^*},$$

so the presence of dephasing reduces the coherence time of the emitted photons. The decay and dephasing rates for a single photon emitter are illustrated in figure 7a.

Dephasing also reduces the indistinguishability between single photons. The indistinguishability is given by the ratio $I = \gamma/(\gamma + \gamma^*)$, so it is desirable to reduce optical dephasing as much as possible. The indistinguishability between photons emitted by a single photon source can be measured by performing a two photon interference experiment where successive photons from the single photon source are interfered on a beamsplitter. If both photons are identical then they will coalesce and exit the final beamsplitter in the same path, an effect known as Hong-Ou-Mandel interference [64]. If the photons are distinguishable, they will be able to exit the beamsplitter along separate paths. In a coincidence counting measurement, the probability of measuring simultaneous clicks between the two detectors is given by $P_{sim} \propto 1 - I$, providing a way to directly characterize the indistinguishability between single photons. We summarize the interplay of the decay and

dephasing rates on the brightness, coherence time, and indistinguishability between the emitted single photons of the source in figure 7b.

3.1.2 Rare-earth ion single photon emission

Rare-earth ions embedded into solid-state hosts possess intra- $4f$ optical transitions that become weakly dipole allowed due to the perturbation of the crystalline lattice. These transitions span a wide range of optical wavelengths depending on the chosen ion and experience minimal electron-phonon coupling due to the relative proximity and confinement of the electrons around the ion nucleus [56]. In fact, the intra- $4f$ optical transitions of rare-earth ions are some of the most pristine known optical transitions in the solid-state. Trivalent erbium (Er^{3+}) is of particular note for quantum networking because it provides optical transitions in the desirable telecom C-band (1530-1565 nm) that experiences the lowest loss for propagation through optical fiber. For example, the lowest energy optical transition for Er^{3+} ($^4I_{13/2} \rightarrow ^4I_{15/2}$) has an optical wavelength of approximately 1550 nm. Operating directly in the telecom window eliminates the need for optical frequency conversion [65–70], which is challenging to achieve in the quantum regime and places extra demands on the overhead required to operate quantum networks.

The weakly allowed $4f - 4f$ optical transitions of rare-earth ions have long excited state lifetimes, T_1 , on the order of 10 ms that lead to long optical coherence times. While these long coherence times are desirable for enabling the distribution of entanglement over long distances, the long lifetimes also consequently lead to a low brightness for individual ions as outlined in section 3.1.1. These low photon emission rates present an immediate challenge for utilizing rare-earth ions as a platform for quantum resource generation by making the optical isolation of single ions particularly difficult.

Initial experiments suggested that isolation of single ions in a crystalline medium could be feasible [71–74], but conclusive optical isolation of single ions was not established until more recently [75–79]. However, these demonstrations of single-ion optical isolation did not collect photons from the lowest lying intra- $4f$ transitions. Rather, they utilized either non-optical methods of detection or optical transitions to higher energy electronic excited states that possess shorter lifetimes. Shorter excited state lifetimes make the higher energy transitions inherently brighter and therefore easier to detect, but also preclude the possibility of exploiting the desirable properties of the lowest lying excited states. Generating single or entangled photons from these transitions is a critical task for building out long distance quantum networks with rare-earth ion doped materials.

3.1.3 Cavity-enhanced optical emission

In order to optically address single ions within the lowest lying $4f - 4f$ transitions, photonic crystal cavities have been utilized to enhance the emission from dilute ensembles of ions as well as resolvable single ions. Enhancement of the optical emission rate has enabled the direct optical observation of single photon emission from the lowest lying optical transitions of rare-earth ions [30, 80–82]. The emission enhancement is manifest by a reduction in the excited state lifetime of the ion by increasing the radiative decay rate by a factor F_P , known as the Purcell factor. The total excited state decay rate for an ion in a cavity then becomes $\gamma' = F_P\gamma_r + \gamma_{nr}$. Placing ions in a cavity enhances their emission rate by increasing the density of electromagnetic states available to the ions for optical decay into the cavity compared to ions in the bulk crystal. This heuristic argument leads to a characterization of the Purcell factor by the relationship

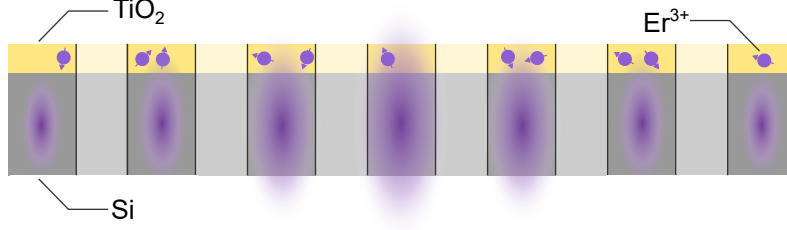


Figure 8: Illustration of a silicon 1D photonic crystal cavity used to enhance the optical emission of erbium ions bound in a TiO_2 film grown on top of silicon.

$$F_P = \frac{3}{4\pi^2} \frac{\lambda^3}{V} Q,$$

where λ is the optical wavelength in the crystal medium, V is the mode volume of the cavity mode, and $Q = \nu/\delta\nu$ is the cavity quality factor. The quality factor is characterized by the ratio of the resonant frequency of the cavity mode, ν , to the full width at half maximum of the cavity mode lineshape, $\delta\nu$. From this relationship it becomes clear that cavities with large quality factors and small mode volumes compared to the scale of the optical wavelength help to produce the greatest emission enhancement. In this regard, the silicon photonics platform is particularly appealing because it enables the fabrication of high quality factor, small mode volume cavities that are otherwise unachievable with bulk or free-space optics. Figure 8 illustrates a device that couples the evanescent cavity field of a 1D silicon photonic crystal cavity to a thin layer of erbium ions above the cavity surface. State-of-the-art measurements have achieved Purcell factors up to 850 for emission from single Er^{3+} ions [82] and radiatively limited single photon emission, where $\gamma' \gg \gamma^*$, has been observed for single Nd^{3+} ions [81]. Crucially, using Purcell enhancement to increase the optical emission rate of single ions also improves the indistinguishability of the emitted photons. An indistinguishability of successively emitted single photons up to $I = 80\%$ has been observed [82]. There is plenty of room for further improvement as well. Photonic crystal cavities with improved design can still significantly increase the achievable Purcell factor through higher cavity quality factors [83] or a reduction of the cavity mode volume [84].

3.1.4 Challenges

One challenge toward realizing a robust source of single photons with rare-earth ion doped materials is the relatively low radiative relaxation rates that lead to low source brightness, as discussed previously in section 3.1.1 and section 3.1.2. This particular challenge can be met by placing the ions inside an optical cavity to enhance the radiative decay rate via the Purcell effect to make single ion detection feasible. Progress in working with Purcell enhanced single ions was covered in section 3.1.3. The long lifetimes of the $4f$ states in rare-earth ions make them particularly sensitive to extra dephasing mechanisms within the crystalline host, which requires Purcell factors $F_P > T_2/T_1$ to realize single photons with a high degree of indistinguishability for quantum networking applications. This challenge can be further compounded by the fabrication of photonic crystal cavities, as the increased proximity to surfaces can introduce spectral wandering and increased optical dephasing. One method to overcome this particular challenge is through passivation of the cavity surfaces [83]. Larger microcavity designs have also been pursued to limit the proximity of ions to the surface [85]. Alternatively, these effects can be mitigated by choosing ions

with an inversion-symmetric lattice site geometry to reduce the sensitivity of the ion to the fluctuating charges near the surface [60].

3.2 Quantum resource storage

3.2.1 Considerations for quantum memories

As outlined in section 2.2, different network architectures are possible that utilize quantum memories based on both single ions and ensembles of ions. Each architecture brings certain benefits. For example, memories based on addressable single ions can ultimately be used to construct quantum repeaters that are error corrected [86], which will be necessary to realize more sophisticated generations of communication networks [38]. On the other hand, memories based on ensembles of ions are particularly useful as they provide a strong interaction with optical photons from the collective action of many ions in the ensemble [47], and are also attractive for multiplexed storage where multiple quantum states can be stored within the same memory [50, 87, 88]. The suitability of a given memory for a particular task can be assessed by the storage time over which the memory can store quantum states, the frequency bandwidth over which the memory can operate, the efficiency with which stored states can be retrieved, and finally the fidelity of the retrieved states to the input state [89]. The utility of a quantum memory is particularly sensitive to storage efficiency and the fidelity of the retrieved state. An efficiency above 1/2 and a fidelity greater than 2/3 are required to operate in the no-cloning regime, such that no better copy the retrieved state can exist [90, 91].

Constructing a memory with an architecture based on rare-earth ions presents several opportunities for storage, both at the single ion level or as an ensemble of ions. Typically, strategies for constructing a single ion memory rely on the spin properties of the ion, while strategies for constructing a memory with an ensemble of ions rely on the optical properties of the ion. In addition to pristine $4f$ - $4f$ optical transitions, rare-earth ions possess electronic ground state levels with long spin lifetimes, capable of reaching the order of minutes [92] to days [93]. In a similar fashion to single photon emission discussed in section 3.1.1, the coherence time of the spin is limited by the spin lifetime such that $T_2 \leq 2T_1$. The storage time over which a spin-based memory can store an arbitrary quantum state is directly proportional to the spin T_2 , so a long spin lifetime is advantageous for the development of quantum memories. Along with their long spin lifetimes, rare-earth ions have demonstrated long spin coherence times [94–97], exceeding 1 second for $^{167}\text{Er}^{3+}$ in a strong magnetic field [94]. The isotope $^{167}\text{Er}^{3+}$ is unique among erbium isotopes in that it possesses a nuclear spin $I = 7/2$, compared to $I = 0$ for all the other stable isotopes of erbium, allowing access to highly coherent hyperfine levels in the presence of a magnetic field. The optical interface provided by the excited states of a rare-earth ion, particularly those within the $4f$ orbital discussed in section 3.1.2, provide a natural interface to map the state of a photon onto the electronic spin state of an ion. In the following sections we will outline the progress that has been achieved with rare-earth ions in both single ion and ensemble memory architectures.

3.2.2 Single rare-earth ion memories

Quantum memories based on single defect centers have proved to be a versatile and powerful resource for various quantum systems [19, 60]. A single electron spin can readily serve as a memory for the state of a single photon. Additionally, the state of an electron spin can be mapped onto a nearby nuclear spin for even longer storage [98, 99] or to enable error correction of the electron spin [100, 101]. Nuclear spins are not naturally sensitive

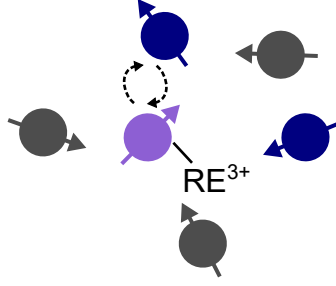


Figure 9: A single rare-earth ion quantum memory. Neighboring nuclear spins (blue) provide an additional resource for long term quantum state storage or even error correction of the electron spin.

to the optical field of the photon and experience a lower noise environment within the solid state crystal than electron spins, making them attractive candidates to serve as long term memory registers and ancilla qubits for the optically sensitive electron spin qubits. A tradeoff in performance between the different spins must be considered, however, since the much narrower nuclear spin transitions can limit the bandwidth of the memory compared to the wider electron spin transitions. Figure 9 illustrates a single rare-earth ion spin in a crystalline host with possible coupling to adjacent nuclear spins.

Rare-earth ions are suitable for memories based on both electron and nuclear spins. The electron spin states of single ions have been optically controlled [78, 82, 102], and spin coherence times for single ions up to 10s of ms have been observed [102]. Electron coherence times of this magnitude are already suitable for linking quantum repeater nodes separated by thousands of km [103], with further improvements in coherence time possible with host lattice engineering discussed below in section 3.2.4. Additionally, single rare-earth ion electron spins have been coupled to adjacent nuclear spins from the host lattice [104–106]. In particular, a single Er^{3+} ion has been used to coherently control a single nuclear spin which served as a register for the electron spin [106], with a SWAP gate fidelity of 87%. While still early in development, these results indicate that single Er^{3+} ions are a versatile resource for quantum networking, as they can pair C-band telecommunications optical transitions with long spin coherence times from both electron and nuclear spins to serve as repeater memory nodes.

3.2.3 Ensemble rare-earth ion memories

Quantum memories based on ensembles of rare-earth ions aim to exploit the inhomogeneous broadening of the optical transitions that are naturally present in ion ensembles in the solid-state. In many rare-earth ion doped materials, the inhomogeneous linewidth of the ensemble can be many orders of magnitude larger than the homogeneous linewidth of a single ion [56]. This ratio makes rare-earth ion ensembles particularly well suited for highly precise spectral shaping using spectral hole burning techniques that can enable multimode quantum memories with a large mode capacity [52].

The method to turn the inhomogeneous ion ensemble into a multimode memory, as noted in section 2.2, is to write an atomic frequency comb into the ensemble with a modulated narrow band laser. The comb consists of multiple narrow absorption peaks with a frequency separation Δ . If a photon with a spectral bandwidth larger than Δ and smaller than the width of the comb is incident on the ensemble, it will be absorbed as a collective excitation of the ions as in equation 8, leading to re-emission at a later time $T = 2\pi/\Delta$ in the form of a photon echo [52, 107]. This basic functionality forms the backbone of atomic frequency comb memories. While the memory described so far provides only a

fixed-duration storage before recall at time T , the echo photon can be recalled on-demand by using an optical control pulse to transfer the collectively excited ions into an auxiliary ground state spin level for storage as a spin wave. Recall of the echo photon from the spin wave can then be made with the application of another control pulse [52, 108].

Atomic frequency comb memories have been used to great effect with rare-earth ion ensembles. Multimode memories have been realized that preserve quantum correlations between highly multiplexed photons stored in the near infrared [109] and telecom [110] bands, where Er^{3+} ions provide storage in the telecom band. Additionally, fidelities of the recalled state to the input state of up to 99.3% have been realized [111], along with qubit storage times up to 10s of ms [112]. Efficiencies of 53% [113] and 56% [114] have been realized for classical input pulses, while efficiencies for quantum light storage up to 27.5% [115] have been realized, all without on-demand recall. Memory efficiency with on-demand recall using spin wave storage has been demonstrated with an efficiency up to 12% [113].

Atomic frequency comb memories are also being explored in nanophotonic platforms [116, 117], critically demonstrating that the protocol is robust even as the physical size of the memory shrinks. The ability to scale the size of quantum memories down from bulk crystals to nanofabricated devices, and especially to devices that can be fabricated with standard semiconductor foundry processes, will be a necessary step to realize repeater networks that span a quantum internet. Improvements to atomic frequency comb memory performance are progressing rapidly and demonstrate the potential for rare-earth ion ensembles to deploy as multimode memories in quantum networks. Here we note that other protocols for building quantum memories with ensembles of ions, such as gradient echo memories [118], electromagnetically induced transparency [119], and off resonant Raman techniques [120] are also being developed, but their multimode capacity can be severely limited by the small size and optical depth of nanophotonic devices. Conversely, the multimode capacity of atomic frequency comb memories is independent of optical depth [52], making the atomic frequency comb protocol appealing for use in state-of-the-art nanophotonic devices.

3.2.4 Challenges

There are still several outstanding challenges toward realizing the goal of widely deployed quantum memories based on rare-earth ion technologies. In particular, the choice of host lattice has a large effect on the spin coherence of the memory, both for single and ensembles of ions. Despite ion ensembles demonstrating memory performance through the atomic frequency comb protocol, which provides storage in the optical transitions, the need for deterministic recall of the echo photons in repeater networks necessitates the use of spin wave storage. The storage time of the spin wave is dictated by the electron spin coherence of the ion. The performance of quantum memories for both single ion and ensemble architectures therefore depend critically on the achievable spin coherence of the ion.

In order to obtain long spin coherence times, such that the spin coherence can approach the lifetime limit, it is advantageous to minimize the interaction of the ion with its host lattice. One route toward achieving this is through the use of non-Kramers ions, which have an even number of electrons with a quenched electronic angular momentum. These ions, including Pr^{3+} and Eu^{3+} , have demonstrated the required long lifetimes and coherence times for use as quantum memories [92, 93, 97, 118, 119, 121, 122], but none of these ions have optical transitions compatible with the telecom transmission band. Kramers ions, such as Nd^{3+} , Er^{3+} , and Yb^{3+} , with an odd number of electrons, are more susceptible to their electromagnetic environment and typically demonstrate shorter spin lifetimes and coherence times as a result. However, Er^{3+} provides critical optical transitions within the

telecom transmission band, making it essential to demonstrate long spin coherence times in spite of the significant electron spin interactions with the host lattice. This challenge demonstrates the need for developing host lattices that can minimize the impact to the electron spin.

The use of host lattices with low densities of paramagnetic impurities and nuclear spins are particularly effective for extending spin coherence [123]. Many common host lattices for rare-earth ions, such as yttrium orthosilicate (Y_2SiO_5 ; YSO), yttrium orthovanadate (YVO_4 ; YVO), and yttrium aluminium garnet ($\text{Y}_3\text{Al}_5\text{O}_{12}$; YAG), often contain residual concentrations of other rare-earth ion dopants and impurities in addition to the desired species and also have a fixed background of yttrium nuclear spins ($I = 1/2$) that cannot be isotopically purified. While impressive demonstrations of spin coherence have been made in these materials, many have required the use of dynamical decoupling sequences or challenging magnetic field configurations which add extra overhead to the memory and limits scalability. This problem is being addressed by a search for materials that can host rare-earth ions with limited or no background spins [124, 125], such as titanium dioxide (TiO_2) [35, 126] and calcium tungstate (CaWO_4) [82, 95] among others. Nanoparticles and molecular crystals are also being considered as potential hosts for rare earth ions [127–129]. As the search for new host crystals progresses, it is important to factor in compatibility with semiconductor foundry processes, so that advances in host selection can leverage the scalable production of semiconductor manufacturing.

An additional challenge for all rare-earth ion based memory architectures is achieving suitable coupling between common single photon sources, such as spontaneous parametric down conversion and four wave mixing sources or semiconductor quantum dots, and the rare-earth device. These sources often have a large bandwidth that contrasts with the typically narrow bandwidth of rare-earth ion systems, leading to reduced efficiency in the storage process. While efficiency can be improved with impedance-matched cavity designs [113–115, 117, 130], the challenge of bandwidth can be addressed in ensemble memories with larger inhomogeneous broadening, particularly by using frequency combs of larger bandwidth [115]. Conversely, these challenges can potentially be met by proper tailoring of the input photons to be stored, or by storing photons produced by rare-earth ion sources [30, 80–82].

3.3 Quantum resource distribution

3.3.1 Considerations for quantum resource distribution and network construction

Quantum resource distribution is the keystone with which quantum networks are ultimately built. The fundamental operation that enables quantum resource distribution is the performance of entanglement swapping operations that create links between remote nodes which were discussed in section 2.3. Quantum resource distribution relies directly on the performance of the repeater as both a source (see sections 2.1 and 3.1) and memory (see sections 2.2 and 3.2), as well as external factors involved with overall network design such as node spacing and the degree of node connectivity. Given the interplay between repeater performance metrics and achievable network design, it is useful to adopt a co-design perspective where the needs of the network at the system level can be used to inform design choices at the device level and vice versa [131].

Despite recent advances in demonstrating a multi-node quantum network enabled by atom-like solid-state systems [132], it remains an outstanding challenge to demonstrate entanglement distribution rates *with* quantum repeaters that exceed the rates possible *without* the use of quantum repeaters [10]. Meeting this challenge will require significant

development in the state-of-the-art for quantum repeater performance, as well as in semiconductor manufacturing capabilities. Increasing the scalability of solid-state quantum platforms to the necessary level, including rare-earth ion based platforms, may require semiconductor foundries that can work with new materials and new process design kits dedicated to quantum device design. In addition to the integration of quantum sources, memories, control and measurement devices in a unified, low-loss platform, it will also be necessary to multiplex the components to achieve useful entanglement rates [87, 88, 133]. These challenges underscore the need for scalable design at the device level informed by network requirements.

Ultimately the success of quantum networks, and rare-earth ion platform for quantum networks in particular, will hinge upon whether or not components and devices can be made reliably at the scale necessary to support the networks. Progress with the fabrication of rare-earth ion devices in platforms compatible with large-scale semiconductor foundry processes suggests that this is possible [21–35]. An important avenue for development to improve achievable entanglement distribution rates is with the development of repeaters based on single rare-earth ions that have the potential to improve rates with increased entanglement swapping probability [134, 135]. Experiments demonstrating single shot readout of individual ions [102, 136], along with multiplexing of individual ions in a single device [137, 138] suggest that there is a path forward for truly scalable rare-earth ion repeaters.

3.3.2 Near-term benchmarks for rare-earth ion enabled quantum networks

In order to support and guide the development of rare-earth ion repeaters for quantum networking, it is useful to determine a set of benchmarks for near-term performance. These benchmarks should be guided by the current state-of-the-art with knowledge of existing material limitations and network capabilities and will help inform benchmarks for longer term development. Here we limit these benchmarks to foundry compatible platforms using single erbium ions, as these are the best candidates for large scale fabrication and interfacing with low-loss optical fiber.

The ultimate goal of constructing a global quantum internet connected by quantum repeaters will likely require the realization of smaller scale networks first. These networks may consist of modular interconnects that connect nodes within a single room, to data center networks or local area networks that connect nodes up to 100s of meters [10, 139]. Addressing networks of this size will be an important step in developing the technologies needed to span more global networks. For these distances, optical and spin coherence times on the order of 10 μ s are suitable for coherent interactions between remote ions and achieving these benchmarks in scalable, nanofabricated devices suitable for the desired networking tasks becomes the challenge. Particularly, developing nanofabricated devices with component efficiencies capable of operating in the no-cloning regime [90, 91] will be critical.

Here we note that optical coherence times up to 10.2 μ s have been observed with a Hahn echo technique for single erbium ions in CaWO_4 coupled to silicon nanocavities, and the same platform has demonstrated electron spin coherence up to 44 μ s also using a Hahn echo technique, likely limited by other paramagnetic impurities in the host crystal [82]. Single cavity coupled erbium ions in Y_2SiO_5 have also been coupled with single neighboring nuclear spins with coherence times up to 1.9 ms [106]. These results demonstrate that erbium ions coupled to nanophotonic structures are capable of reaching the necessary coherence times for local network applications. The primary roadblock to scalability is the bulk crystal used to house the ions. Demonstrations of optical and spin coherence times up

to 10 μs in a platform that eliminates the need for the bulk crystal would enable rare-earth ion technologies to begin addressing the needs of networks at this scale. Developing global scale quantum networks will require broad based advances in both hardware, software, and network design structures that will continue to happen over a longer time period (likely exceeding 10 years) [10, 11]. We expect that advances in scalable rare-earth ion platforms today will have significant impact on the development of these larger networks.

4 Perspectives

The development of a fully scalable quantum repeater will enable the growth of quantum networks with nodes spanning 100s of km or more, which will form the backbone of a quantum internet. Quantum repeaters require the ability to faithfully generate, store, and distribute entanglement between the network nodes, and rare-earth ions embedded in solid-state hosts, particularly hosts compatible with large scale semiconductor manufacturing, are an attractive platform to meet these requirements. We have drawn special attention to erbium in this review because it provides a natural interface with low-loss optical telecommunications networks operating near 1550 nm. Of particular near-term importance will be the development of erbium ion devices in a scalable platform that can achieve optical and spin coherence times on the order of 10 μs . This will enable quantum networks at the local level with nodes that span up to 100s of meters, spurring continued innovation in quantum networking technologies. The continued development of rare-earth ion technologies in scalable platforms has the capability to bring budding quantum networks to fruition.

Taking a broader view, the large ecosystem of quantum technologies presents additional challenges and opportunities. Quantum computers and quantum sensors are all being developed with different and often incompatible platforms, from superconducting and spin qubits operating at mK temperatures and GHz frequencies, to trapped ion and atom systems operating in ultra-high vacuum and frequencies of 100s of THz. In order to build robust and versatile networks capable of harnessing the best qualities of each system, it will be necessary to establish ways to form interconnects between them [10, 139].

A particular interconnect, the quantum state transducer, would be capable of mapping the quantum state of a qubit in one platform onto a qubit in a separate platform and vice versa. The importance of connecting quantum devices to fiber networks for long range networking means one of these platforms is often required to be an optical photon with a wavelength near 1550 nm to access the low-loss telecom transmission window. A solution for quantum state transduction between the microwave and telecom optical regimes [140] is critically needed for superconducting [141] and spin [142] qubit platforms for quantum computing.

Rare-earth ion systems may play a significant role in this regard since they possess highly coherent microwave and optical frequency transitions. Schemes to realize microwave to optical transducers with high efficiency using rare-earth ions have been proposed [143, 144] and experiments are actively pursuing the goal [145–148]. The promise of quantum state transducers using rare-earth ions indicates that the rare-earth ion platform is not only attractive for developing the quantum repeaters necessary to build out global quantum networks, but also for providing a means to expand the reach of the network to other diverse qubit platforms and technologies. This expanded toolkit will ultimately lead to more functional quantum networks by allowing qubits of different types to interact within the same network. Rare-earth ions are therefore well positioned to play a significant role in a future quantum internet.

Acknowledgments

Work by S.E.S. and M.K.S. was carried out at Argonne National Laboratory with support from the US Department of Energy Office of Science Advanced Scientific Computing Research program under CRADA A22112 through the Chain Reaction Innovations program. The authors would like to further acknowledge helpful conversations with Christophe Jurczak and Xavier Aubry.

References

- [1] Stephanie Wehner, David Elkouss, and Ronald Hanson. “Quantum internet: A vision for the road ahead”. *Science* **362**, eaam9288 (2018).
- [2] Christoph Simon. “Towards a global quantum network”. *Nature Photon* **11**, 678–680 (2017).
- [3] H. J. Kimble. “The quantum internet”. *Nature* **453**, 1023–1030 (2008).
- [4] Feihu Xu, Xiongfeng Ma, Qiang Zhang, Hoi-Kwong Lo, and Jian-Wei Pan. “Secure quantum key distribution with realistic devices”. *Rev. Mod. Phys.* **92**, 025002 (2020).
- [5] P. Kómár, E. M. Kessler, M. Bishof, L. Jiang, A. S. Sørensen, J. Ye, and M. D. Lukin. “A quantum network of clocks”. *Nature Phys* **10**, 582–587 (2014).
- [6] Daniel Gottesman, Thomas Jennewein, and Sarah Croke. “Longer-Baseline Telescopes Using Quantum Repeaters”. *Phys. Rev. Lett.* **109**, 070503 (2012).
- [7] David Rideout, Thomas Jennewein, Giovanni Amelino-Camelia, Tommaso F. Demarie, Brendon L. Higgins, Achim Kempf, Adrian Kent, Raymond Laflamme, Xian Ma, Robert B. Mann, Eduardo Martín-Martínez, Nicolas C. Menicucci, John Moffat, Christoph Simon, Rafael Sorkin, Lee Smolin, and Daniel R. Terno. “Fundamental quantum optics experiments conceivable with satellites—reaching relativistic distances and velocities”. *Class. Quantum Grav.* **29**, 224011 (2012).
- [8] R. Ursin, F. Tiefenbacher, T. Schmitt-Manderbach, H. Weier, T. Scheidl, M. Lindenthal, B. Blauensteiner, T. Jennewein, J. Perdigues, P. Trojek, B. Ömer, M. Fürst, M. Meyenburg, J. Rarity, Z. Sodnik, C. Barbieri, H. Weinfurter, and A. Zeilinger. “Entanglement-based quantum communication over 144 km”. *Nature Phys* **3**, 481–486 (2007).
- [9] Juan Yin, Yuan Cao, Yu-Huai Li, Sheng-Kai Liao, Liang Zhang, Ji-Gang Ren, Wen-Qi Cai, Wei-Yue Liu, Bo Li, Hui Dai, Guang-Bing Li, Qi-Ming Lu, Yun-Hong Gong, Yu Xu, Shuang-Lin Li, Feng-Zhi Li, Ya-Yun Yin, Zi-Qing Jiang, Ming Li, Jian-Jun Jia, Ge Ren, Dong He, Yi-Lin Zhou, Xiao-Xiang Zhang, Na Wang, Xiang Chang, Zhen-Cai Zhu, Nai-Le Liu, Yu-Ao Chen, Chao-Yang Lu, Rong Shu, Cheng-Zhi Peng, Jian-Yu Wang, and Jian-Wei Pan. “Satellite-based entanglement distribution over 1200 kilometers”. *Science* **356**, 1140–1144 (2017).
- [10] David D. Awschalom, Hannes Bernien, Rex Brown, Aashish Clerk, Eric Chitambar, Alan Dibos, Jennifer Dionne, Mark Eriksson, Bill Fefferman, Greg David Fuchs, Jay Gambetta, Elizabeth Goldschmidt, Supratik Guha, F. Joseph Heremans, Kent David Irwin, Ania Bleszynski Jayich, Liang Jiang, Jonathan Karsch, Mark Kasevich, Shimon Kolkowitz, Paul G. Kwiat, Thaddeus Ladd, Jay Lowell, Dmitri Maslov, Nadya Mason, Anne Y. Matsuura, Robert McDermott, Rod van Meter, Aaron Miller, Jason Orcutt, Mark Saffman, Monika Schleier-Smith, Manish Kumar Singh, Phil Smith, Martin Suchara, Farzam Toudeh-Fallah, Matt Turlington, Benjamin Woods, and Tian Zhong. “A Roadmap for Quantum Interconnects”. *Technical Report ANL-22/83*. Argonne National Lab. (ANL), Argonne, IL (United States) (2022).

- [11] David Awschalom. “From Long-distance Entanglement to Building a Nationwide Quantum Internet: Report of the DOE Quantum Internet Blueprint Workshop”. [Technical Report BNL-216179-2020-FORE](#). Brookhaven National Lab. (BNL), Upton, NY (United States) (2020).
- [12] M. Peev, C. Pacher, R. Alléaume, C. Barreiro, J. Bouda, W. Boxleitner, T. Debuisschert, E. Diamanti, M. Dianati, J. F. Dynes, S. Fasel, S. Fossier, M. Fürst, J.-D. Gautier, O. Gay, N. Gisin, P. Grangier, A. Happe, Y. Hasani, M. Hentschel, H. Hübel, G. Humer, T. Länger, M. Legré, R. Lieger, J. Lodewyck, T. Lorünser, N. Lütkenhaus, A. Marhold, T. Matyus, O. Maurhart, L. Monat, S. Nauerth, J.-B. Page, A. Poppe, E. Querasser, G. Ribordy, S. Robyr, L. Salvail, A. W. Sharpe, A. J. Shields, D. Stucki, M. Suda, C. Tamas, T. Themel, R. T. Thew, Y. Thoma, A. Treiber, P. Trinkler, R. Tualle-Brouiri, F. Vannel, N. Walenta, H. Weier, H. Weinfurter, I. Wimberger, Z. L. Yuan, H. Zbinden, and A. Zeilinger. “The SECOQC quantum key distribution network in Vienna”. [New J. Phys.](#) **11**, 075001 (2009).
- [13] D. Stucki, M. Legré, F. Buntschu, B. Clausen, N. Felber, N. Gisin, L. Henzen, P. Junod, G. Litzistorf, P. Monbaron, L. Monat, J.-B. Page, D. Perroud, G. Ribordy, A. Rochas, S. Robyr, J. Tavares, R. Thew, P. Trinkler, S. Ventura, R. Voinol, N. Walenta, and H. Zbinden. “Long-term performance of the SwissQuantum quantum key distribution network in a field environment”. [New J. Phys.](#) **13**, 123001 (2011).
- [14] M. Sasaki, M. Fujiwara, H. Ishizuka, W. Klaus, K. Wakui, M. Takeoka, S. Miki, T. Yamashita, Z. Wang, A. Tanaka, K. Yoshino, Y. Nambu, S. Takahashi, A. Tajima, A. Tomita, T. Domeki, T. Hasegawa, Y. Sakai, H. Kobayashi, T. Asai, K. Shimizu, T. Tokura, T. Tsurumaru, M. Matsui, T. Honjo, K. Tamaki, H. Takesue, Y. Tokura, J. F. Dynes, A. R. Dixon, A. W. Sharpe, Z. L. Yuan, A. J. Shields, S. Uchikoga, M. Legré, S. Robyr, P. Trinkler, L. Monat, J.-B. Page, G. Ribordy, A. Poppe, A. Allacher, O. Maurhart, T. Länger, M. Peev, and A. Zeilinger. “Field test of quantum key distribution in the Tokyo QKD Network”. [Opt. Express](#), **OE 19**, 10387–10409 (2011).
- [15] Yingqiu Mao, Bi-Xiao Wang, Chunxu Zhao, Guangquan Wang, Ruichun Wang, Honghai Wang, Fei Zhou, Jimin Nie, Qing Chen, Yong Zhao, Qiang Zhang, Jun Zhang, Teng-Yun Chen, and Jian-Wei Pan. “Integrating quantum key distribution with classical communications in backbone fiber network”. [Opt. Express](#), **OE 26**, 6010–6020 (2018).
- [16] J. F. Dynes, A. Wonfor, W. W.-S. Tam, A. W. Sharpe, R. Takahashi, M. Lucamarini, A. Plews, Z. L. Yuan, A. R. Dixon, J. Cho, Y. Tanizawa, J.-P. Elbers, H. Greißer, I. H. White, R. V. Penty, and A. J. Shields. “Cambridge quantum network”. [npj Quantum Inf](#) **5**, 1–8 (2019).
- [17] W. K. Wootters and W. H. Zurek. “A single quantum cannot be cloned”. [Nature](#) **299**, 802–803 (1982).
- [18] Igor Aharonovich, Dirk Englund, and Milos Toth. “Solid-state single-photon emitters”. [Nature Photon](#) **10**, 631–641 (2016).
- [19] David D. Awschalom, Ronald Hanson, Jörg Wrachtrup, and Brian B. Zhou. “Quantum technologies with optically interfaced solid-state spins”. [Nature Photon](#) **12**, 516–527 (2018).
- [20] F. De Martini, G. Innocenti, G. R. Jacobovitz, and P. Mataloni. “Anomalous Spontaneous Emission Time in a Microscopic Optical Cavity”. [Phys. Rev. Lett.](#) **59**, 2955–2958 (1987).
- [21] H. Przybylinska, W. Jantsch, Yu. Suprun-Belevitch, M. Stepikhova, L. Palmetshofer, G. Hendorfer, A. Kozanecki, R. J. Wilson, and B. J. Sealy. “Optically active erbium centers in silicon”. [Phys. Rev. B](#) **54**, 2532–2547 (1996).

- [22] A. J. Kenyon. “Erbium in silicon”. *Semicond. Sci. Technol.* **20**, R65 (2005).
- [23] Lorenz Weiss, Andreas Gritsch, Benjamin Merkel, and Andreas Reiserer. “Erbium dopants in nanophotonic silicon waveguides”. *Optica, OPTICA* **8**, 40–41 (2021).
- [24] Andreas Gritsch, Lorenz Weiss, Johannes Früh, Stephan Rinner, and Andreas Reiserer. “Narrow Optical Transitions in Erbium-Implanted Silicon Waveguides”. *Phys. Rev. X* **12**, 041009 (2022).
- [25] Ian R. Berkman, Alexey Lyasota, Gabriele G. de Boo, John G. Bartholomew, Brett C. Johnson, Jeffrey C. McCallum, Bin-Bin Xu, Shouyi Xie, Rose L. Ahlefeldt, Matthew J. Sellars, Chunming Yin, and Sven Rogge. “Observing Er^{3+} Sites in Si With an In Situ Single-Photon Detector”. *Phys. Rev. Appl.* **19**, 014037 (2023).
- [26] M. U. Staudt, M. Afzelius, H. de Riedmatten, S. R. Hastings-Simon, C. Simon, R. Ricken, H. Suche, W. Sohler, and N. Gisin. “Interference of Multimode Photon Echoes Generated in Spatially Separated Solid-State Atomic Ensembles”. *Phys. Rev. Lett.* **99**, 173602 (2007).
- [27] N. Sinclair, E. Saglamyurek, M. George, R. Ricken, C. La Mela, W. Sohler, and W. Tittel. “Spectroscopic investigations of a Ti:Tm:LiNbO_3 waveguide for photon-echo quantum memory”. *Journal of Luminescence* **130**, 1586–1593 (2010).
- [28] Erhan Saglamyurek, Neil Sinclair, Jeongwan Jin, Joshua A. Slater, Daniel Oblak, Félix Bussi eres, Mathew George, Raimund Ricken, Wolfgang Sohler, and Wolfgang Tittel. “Broadband waveguide quantum memory for entangled photons”. *Nature* **469**, 512–515 (2011).
- [29] Subhojit Dutta, Elizabeth A. Goldschmidt, Sabyasachi Barik, Uday Saha, and Edo Waks. “Integrated Photonic Platform for Rare-Earth Ions in Thin Film Lithium Niobate”. *Nano Lett.* **20**, 741–747 (2020).
- [30] Likai Yang, Sihao Wang, Mohan Shen, Jiacheng Xie, and Hong X. Tang. “Controlling single rare earth ion emission in an electro-optical nanocavity” (2022). [arxiv:2211.12449](https://arxiv.org/abs/2211.12449).
- [31] Yiyang Gong, Maria Makarova, Sel uk Yerci, Rui Li, Martin J. Stevens, Burm Baek, Sae Woo Nam, Robert H. Hadfield, Sander N. Dorenbos, Val Zwiller, Jelena Vu kovi , and Luca Dal Negro. “Linewidth narrowing and Purcell enhancement in photonic crystal cavities on an Er-doped silicon nitride platform”. *Opt. Express, OE* **18**, 2601–2612 (2010).
- [32] Yiyang Gong, Maria Makarova, Sel uk Yerci, Rui Li, Martin J. Stevens, Burm Baek, Sae Woo Nam, Luca Dal Negro, and Jelena Vu kovi . “Observation of Transparency of Erbium-doped Silicon nitride in photonic crystal nanobeam cavities”. *Opt. Express, OE* **18**, 13863–13873 (2010).
- [33] Dapeng Ding, Lino M. C. Pereira, Jared F. Bauters, Martijn J. R. Heck, Gesa Welker, Andr  Vantomme, John E. Bowers, Michiel J. A. de Dood, and Dirk Bouwmeester. “Multidimensional Purcell effect in an ytterbium-doped ring resonator”. *Nature Photon* **10**, 385–388 (2016).
- [34] Manish Kumar Singh, Abhinav Prakash, Gary Wolfowicz, Jianguo Wen, Yizhong Huang, Tijana Rajh, David D. Awschalom, Tian Zhong, and Supratik Guha. “Epitaxial Er-doped Y_2O_3 on silicon for quantum coherent devices”. *APL Materials* **8**, 031111 (2020).
- [35] Alan M. Dibos, Michael T. Solomon, Sean E. Sullivan, Manish K. Singh, Kathryn E. Sautter, Connor P. Horn, Gregory D. Grant, Yulin Lin, Jianguo Wen, F. Joseph Heremans, Supratik Guha, and David D. Awschalom. “Purcell Enhancement of Erbium Ions in TiO_2 on Silicon Nanocavities”. *Nano Lett.* **22**, 6530–6536 (2022).

- [36] W. Dür, H.-J. Briegel, J. I. Cirac, and P. Zoller. “Quantum repeaters based on entanglement purification”. *Phys. Rev. A* **59**, 169–181 (1999).
- [37] Sreraman Muralidharan, Jungsang Kim, Norbert Lütkenhaus, Mikhail D. Lukin, and Liang Jiang. “Ultrafast and Fault-Tolerant Quantum Communication across Long Distances”. *Phys. Rev. Lett.* **112**, 250501 (2014).
- [38] Sreraman Muralidharan, Linshu Li, Jungsang Kim, Norbert Lütkenhaus, Mikhail D. Lukin, and Liang Jiang. “Optimal architectures for long distance quantum communication”. *Sci Rep* **6**, 20463 (2016).
- [39] L.-M. Duan and C. Monroe. “Colloquium: Quantum networks with trapped ions”. *Rev. Mod. Phys.* **82**, 1209–1224 (2010).
- [40] C. Monroe and J. Kim. “Scaling the Ion Trap Quantum Processor”. *Science* **339**, 1164–1169 (2013).
- [41] Robert Raussendorf and Hans J. Briegel. “A One-Way Quantum Computer”. *Phys. Rev. Lett.* **86**, 5188–5191 (2001).
- [42] H. J. Briegel, D. E. Browne, W. Dür, R. Raussendorf, and M. Van den Nest. “Measurement-based quantum computation”. *Nature Phys* **5**, 19–26 (2009).
- [43] H.-J. Briegel, W. Dür, J. I. Cirac, and P. Zoller. “Quantum Repeater: The Role of Imperfect Local Operations in Quantum Communication”. *Phys. Rev. Lett.* **81**, 5932–5935 (1998).
- [44] S. Bose, P. L. Knight, M. B. Plenio, and V. Vedral. “Proposal for Teleportation of an Atomic State via Cavity Decay”. *Phys. Rev. Lett.* **83**, 5158–5161 (1999).
- [45] Sean D. Barrett and Pieter Kok. “Efficient high-fidelity quantum computation using matter qubits and linear optics”. *Phys. Rev. A* **71**, 060310 (2005).
- [46] Andreas Reiserer and Gerhard Rempe. “Cavity-based quantum networks with single atoms and optical photons”. *Rev. Mod. Phys.* **87**, 1379–1418 (2015).
- [47] L.-M. Duan, M. D. Lukin, J. I. Cirac, and P. Zoller. “Long-distance quantum communication with atomic ensembles and linear optics”. *Nature* **414**, 413–418 (2001).
- [48] Yang Wang, Alexander N. Craddock, Rourke Sekelsky, Mael Flament, and Mehdi Namazi. “Field-Deployable Quantum Memory for Quantum Networking”. *Phys. Rev. Appl.* **18**, 044058 (2022).
- [49] Mingtao Cao, Félix Hoffet, Shuwei Qiu, Alexandra S. Sheremet, and Julien Laurat. “Efficient reversible entanglement transfer between light and quantum memories”. *Optica*, *OPTICA* **7**, 1440–1444 (2020).
- [50] Nicolas Sangouard, Christoph Simon, Hugues de Riedmatten, and Nicolas Gisin. “Quantum repeaters based on atomic ensembles and linear optics”. *Rev. Mod. Phys.* **83**, 33–80 (2011).
- [51] Nicolas Sangouard, Christoph Simon, Mikael Afzelius, and Nicolas Gisin. “Analysis of a quantum memory for photons based on controlled reversible inhomogeneous broadening”. *Phys. Rev. A* **75**, 032327 (2007).
- [52] Mikael Afzelius, Christoph Simon, Hugues de Riedmatten, and Nicolas Gisin. “Multimode quantum memory based on atomic frequency combs”. *Phys. Rev. A* **79**, 052329 (2009).
- [53] Dario Lago-Rivera, Samuele Grandi, Jelena V. Rakonjac, Alessandro Seri, and Hugues de Riedmatten. “Telecom-heralded entanglement between multimode solid-state quantum memories”. *Nature* **594**, 37–40 (2021).
- [54] G. H. Dieke and H. M. Crosswhite. “The Spectra of the Doubly and Triply Ionized Rare Earths”. *Appl. Opt.*, *AO* **2**, 675–686 (1963).
- [55] Roger M Macfarlane. “High-resolution laser spectroscopy of rare-earth doped insulators: A personal perspective”. *Journal of Luminescence* **100**, 1–20 (2002).

- [56] C. W. Thiel, Thomas Böttger, and R. L. Cone. “Rare-earth-doped materials for applications in quantum information storage and signal processing”. *Journal of Luminescence* **131**, 353–361 (2011).
- [57] Axel Kuhn, Markus Hennrich, and Gerhard Rempe. “Deterministic Single-Photon Source for Distributed Quantum Networking”. *Phys. Rev. Lett.* **89**, 067901 (2002).
- [58] Xiang Guo, Chang-ling Zou, Carsten Schuck, Hojoong Jung, Risheng Cheng, and Hong X. Tang. “Parametric down-conversion photon-pair source on a nanophotonic chip”. *Light Sci Appl* **6**, e16249–e16249 (2017).
- [59] S. Paesani, M. Borghi, S. Signorini, A. Maïnos, L. Pavesi, and A. Laing. “Near-ideal spontaneous photon sources in silicon quantum photonics”. *Nat Commun* **11**, 2505 (2020).
- [60] Gary Wolfowicz, F. Joseph Heremans, Christopher P. Anderson, Shun Kanai, Hosung Seo, Adam Gali, Giulia Galli, and David D. Awschalom. “Quantum guidelines for solid-state spin defects”. *Nat Rev Mater* **6**, 906–925 (2021).
- [61] Lee C. Bassett, Audrius Alkauskas, Annemarie L. Exarhos, and Kai-Mei C. Fu. “Quantum defects by design”. *Nanophotonics* **8**, 1867–1888 (2019).
- [62] Lukas Hanschke, Kevin A. Fischer, Stefan Appel, Daniil Lukin, Jakob Wierzbowski, Shuo Sun, Rahul Trivedi, Jelena Vučković, Jonathan J. Finley, and Kai Müller. “Quantum dot single-photon sources with ultra-low multi-photon probability”. *npj Quantum Inf* **4**, 1–6 (2018).
- [63] Thomas Böttger, C. W. Thiel, Y. Sun, and R. L. Cone. “Optical decoherence and spectral diffusion at 1.5 μm in $\text{Er}^{3+} : \text{Y}_2\text{SiO}_5$ versus magnetic field, temperature, and Er^{3+} concentration”. *Phys. Rev. B* **73**, 075101 (2006).
- [64] Rodney Loudon. “Multimode and continuous-mode quantum optics”. In *The Quantum Theory of Light*. Pages 233–287. Oxford University Press, Oxford ; New York (2000). 3rd edition.
- [65] Prem Kumar. “Quantum frequency conversion”. *Opt. Lett., OL* **15**, 1476–1478 (1990).
- [66] Jianming Huang and Prem Kumar. “Observation of quantum frequency conversion”. *Phys. Rev. Lett.* **68**, 2153–2156 (1992).
- [67] A. G. Radnaev, Y. O. Dudin, R. Zhao, H. H. Jen, S. D. Jenkins, A. Kuzmich, and T. a. B. Kennedy. “A quantum memory with telecom-wavelength conversion”. *Nature Phys* **6**, 894–899 (2010).
- [68] Xiang Guo, Chang-Ling Zou, Hojoong Jung, and Hong X. Tang. “On-Chip Strong Coupling and Efficient Frequency Conversion between Telecom and Visible Optical Modes”. *Phys. Rev. Lett.* **117**, 123902 (2016).
- [69] Matthias Bock, Pascal Eich, Stephan Kucera, Matthias Kreis, Andreas Lenhard, Christoph Becher, and Jürgen Eschner. “High-fidelity entanglement between a trapped ion and a telecom photon via quantum frequency conversion”. *Nat Commun* **9**, 1998 (2018).
- [70] Anshuman Singh, Qing Li, Shunfa Liu, Ying Yu, Xiyuan Lu, Christian Schneider, Sven Höfling, John Lawall, Varun Verma, Richard Mirin, Sae Woo Nam, Jin Liu, and Kartik Srinivasan. “Quantum frequency conversion of a quantum dot single-photon source on a nanophotonic chip”. *Optica, OPTICA* **6**, 563–569 (2019).
- [71] R. Lange, W. Grill, and W. Martienssen. “Observation of Single Impurity Ions in a Crystal”. *EPL* **6**, 499 (1988).
- [72] R. Rodrigues-Herzog, F. Trotta, H. Bill, J.-M. Segura, B. Hecht, and H.-J. Güntherodt. “Optical microscopy of single ions and morphological inhomogeneities in Sm-doped CaF_2 thin films”. *Phys. Rev. B* **62**, 11163–11169 (2000).

- [73] Andrew P Bartko, Lynn A Peyser, Robert M Dickson, A Mehta, T Thundat, R Bhargava, and M. D Barnes. “Observation of dipolar emission patterns from isolated $\text{Eu}^{3+}:\text{Y}_2\text{O}_3$ doped nanocrystals: New evidence for single ion luminescence”. *Chemical Physics Letters* **358**, 459–465 (2002).
- [74] Yu. V. Malyukin, A. A. Masalov, and P. N. Zhmurin. “Single-ion fluorescence spectroscopy of a $\text{Y}_2\text{SiO}_5:\text{Pr}^{3+}$ nanocluster”. *Physics Letters A* **316**, 147–152 (2003).
- [75] R. Kolesov, K. Xia, R. Reuter, R. Stöhr, A. Zappe, J. Meijer, P. R. Hemmer, and J. Wrachtrup. “Optical detection of a single rare-earth ion in a crystal”. *Nat Commun* **3**, 1029 (2012).
- [76] Chunming Yin, Milos Rancic, Gabriele G. de Boo, Nikolas Stavrias, Jeffrey C. McCallum, Matthew J. Sellars, and Sven Rogge. “Optical addressing of an individual erbium ion in silicon”. *Nature* **497**, 91–94 (2013).
- [77] Ippei Nakamura, Tatsuya Yoshihiro, Hironori Inagawa, Satoru Fujiyoshi, and Michio Matsushita. “Spectroscopy of single Pr^{3+} ion in LaF_3 crystal at 1.5 K”. *Sci Rep* **4**, 7364 (2014).
- [78] P. Siyushev, K. Xia, R. Reuter, M. Jamali, N. Zhao, N. Yang, C. Duan, N. Kukharchyk, A. D. Wieck, R. Kolesov, and J. Wrachtrup. “Coherent properties of single rare-earth spin qubits”. *Nat Commun* **5**, 3895 (2014).
- [79] T. Utikal, E. Eichhammer, L. Petersen, A. Renn, S. Götzinger, and V. Sandoghdar. “Spectroscopic detection and state preparation of a single praseodymium ion in a crystal”. *Nat Commun* **5**, 3627 (2014).
- [80] A. M. Dibos, M. Raha, C. M. Phenicie, and J. D. Thompson. “Atomic Source of Single Photons in the Telecom Band”. *Phys. Rev. Lett.* **120**, 243601 (2018).
- [81] Tian Zhong, Jonathan M. Kindem, John G. Bartholomew, Jake Rochman, Ioana Craiciu, Varun Verma, Sae Woo Nam, Francesco Marsili, Matthew D. Shaw, Andrew D. Beyer, and Andrei Faraon. “Optically Addressing Single Rare-Earth Ions in a Nanophotonic Cavity”. *Phys. Rev. Lett.* **121**, 183603 (2018).
- [82] Salim Ourari, Łukasz Dusanowski, Sebastian P. Horvath, Mehmet T. Uysal, Christopher M. Phenicie, Paul Stevenson, Mouktik Raha, Songtao Chen, Robert J. Cava, Nathalie P. de Leon, and Jeff D. Thompson. “Indistinguishable telecom band photons from a single erbium ion in the solid state” (2023). [arxiv:2301.03564](https://arxiv.org/abs/2301.03564).
- [83] Takashi Asano, Yoshiaki Ochi, Yasushi Takahashi, Katsuhiro Kishimoto, and Susumu Noda. “Photonic crystal nanocavity with a Q factor exceeding eleven million”. *Opt. Express*, OE **25**, 1769–1777 (2017).
- [84] Shuren Hu and Sharon M. Weiss. “Design of Photonic Crystal Cavities for Extreme Light Concentration”. *ACS Photonics* **3**, 1647–1653 (2016).
- [85] Benjamin Merkel, Alexander Ulanowski, and Andreas Reiserer. “Coherent and Purcell-Enhanced Emission from Erbium Dopants in a Cryogenic High-Q Resonator”. *Phys. Rev. X* **10**, 041025 (2020).
- [86] J. J. Longdell, M. J. Sellars, and N. B. Manson. “Demonstration of Conditional Quantum Phase Shift Between Ions in a Solid”. *Phys. Rev. Lett.* **93**, 130503 (2004).
- [87] Christoph Simon, Hugues de Riedmatten, Mikael Afzelius, Nicolas Sangouard, Hugo Zbinden, and Nicolas Gisin. “Quantum Repeaters with Photon Pair Sources and Multimode Memories”. *Phys. Rev. Lett.* **98**, 190503 (2007).
- [88] O. A. Collins, S. D. Jenkins, A. Kuzmich, and T. A. B. Kennedy. “Multiplexed Memory-Insensitive Quantum Repeaters”. *Phys. Rev. Lett.* **98**, 060502 (2007).
- [89] Alexander I. Lvovsky, Barry C. Sanders, and Wolfgang Tittel. “Optical quantum memory”. *Nature Photon* **3**, 706–714 (2009).

- [90] Frédéric Grosshans and Philippe Grangier. “Quantum cloning and teleportation criteria for continuous quantum variables”. *Phys. Rev. A* **64**, 010301 (2001).
- [91] S. Massar and S. Popescu. “Optimal Extraction of Information from Finite Quantum Ensembles”. *Phys. Rev. Lett.* **74**, 1259–1263 (1995).
- [92] Keith Holliday, Mauro Croci, Eric Vauthey, and Urs P. Wild. “Spectral hole burning and holography in an $\text{Y}_2\text{SiO}_5\text{:Pr}^{3+}$ crystal”. *Phys. Rev. B* **47**, 14741–14752 (1993).
- [93] Flurin Könz, Y. Sun, C. W. Thiel, R. L. Cone, R. W. Equall, R. L. Hutcheson, and R. M. Macfarlane. “Temperature and concentration dependence of optical dephasing, spectral-hole lifetime, and anisotropic absorption in $\text{Eu}^{3+}\text{:Y}_2\text{SiO}_5$ ”. *Phys. Rev. B* **68**, 085109 (2003).
- [94] Miloš Rančić, Morgan P. Hedges, Rose L. Ahlefeldt, and Matthew J. Sellars. “Coherence time of over a second in a telecom-compatible quantum memory storage material”. *Nature Phys* **14**, 50–54 (2018).
- [95] Marianne Le Dantec, Miloš Rančić, Sen Lin, Eric Billaud, Vishal Ranjan, Daniel Flanigan, Sylvain Bertaina, Thierry Chanelière, Philippe Goldner, Andreas Erb, Ren Bao Liu, Daniel Estève, Denis Vion, Emmanuel Flurin, and Patrice Bertet. “Twenty-three-millisecond electron spin coherence of erbium ions in a natural-abundance crystal”. *Science Advances* **7**, eabj9786 (2021).
- [96] Antonio Ortu, Alexey Tiranov, Sacha Welinski, Florian Fröwis, Nicolas Gisin, Alban Ferrier, Philippe Goldner, and Mikael Afzelius. “Simultaneous coherence enhancement of optical and microwave transitions in solid-state electronic spins”. *Nature Mater* **17**, 671–675 (2018).
- [97] E. Fraval, M. J. Sellars, and J. J. Longdell. “Method of Extending Hyperfine Coherence Times in $\text{Pr}^{3+}\text{:Y}_2\text{SiO}_5$ ”. *Phys. Rev. Lett.* **92**, 077601 (2004).
- [98] M. V. Gurudev Dutt, L. Childress, L. Jiang, E. Togan, J. Maze, F. Jelezko, A. S. Zibrov, P. R. Hemmer, and M. D. Lukin. “Quantum Register Based on Individual Electronic and Nuclear Spin Qubits in Diamond”. *Science* **316**, 1312–1316 (2007).
- [99] G. D. Fuchs, G. Burkard, P. V. Klimov, and D. D. Awschalom. “A quantum memory intrinsic to single nitrogen–vacancy centres in diamond”. *Nature Phys* **7**, 789–793 (2011).
- [100] T. H. Taminiau, J. Cramer, T. van der Sar, V. V. Dobrovitski, and R. Hanson. “Universal control and error correction in multi-qubit spin registers in diamond”. *Nature Nanotech* **9**, 171–176 (2014).
- [101] G. Waldherr, Y. Wang, S. Zaiser, M. Jamali, T. Schulte-Herbrüggen, H. Abe, T. Ohshima, J. Isoya, J. F. Du, P. Neumann, and J. Wrachtrup. “Quantum error correction in a solid-state hybrid spin register”. *Nature* **506**, 204–207 (2014).
- [102] Jonathan M. Kindem, Andrei Ruskuc, John G. Bartholomew, Jake Rochman, Yan Qi Huan, and Andrei Faraon. “Control and single-shot readout of an ion embedded in a nanophotonic cavity”. *Nature* **580**, 201–204 (2020).
- [103] M. Razavi, M. Piani, and N. Lütkenhaus. “Quantum repeaters with imperfect memories: Cost and scalability”. *Phys. Rev. A* **80**, 032301 (2009).
- [104] Thomas Kornher, Da-Wu Xiao, Kangwei Xia, Fiammetta Sardi, Nan Zhao, Roman Kolesov, and Jörg Wrachtrup. “Sensing Individual Nuclear Spins with a Single Rare-Earth Electron Spin”. *Phys. Rev. Lett.* **124**, 170402 (2020).
- [105] Andrei Ruskuc, Chun-Ju Wu, Jake Rochman, Joonhee Choi, and Andrei Faraon. “Nuclear spin-wave quantum register for a solid-state qubit”. *Nature* **602**, 408–413 (2022).
- [106] Mehmet T. Uysal, Mouktik Raha, Songtao Chen, Christopher M. Phenicie, Salim Ourari, Mengen Wang, Chris G. Van de Walle, Viatcheslav V. Dobrovitski, and

- Jeff D. Thompson. “Coherent Control of a Nuclear Spin via Interactions with a Rare-Earth Ion in the Solid State”. *PRX Quantum* **4**, 010323 (2023).
- [107] Hugues de Riedmatten, Mikael Afzelius, Matthias U. Staudt, Christoph Simon, and Nicolas Gisin. “A solid-state light–matter interface at the single-photon level”. *Nature* **456**, 773–777 (2008).
- [108] Mikael Afzelius, Imam Usmani, Atia Amari, Björn Lauritzen, Andreas Walther, Christoph Simon, Nicolas Sangouard, Jiří Minář, Hugues de Riedmatten, Nicolas Gisin, and Stefan Kröll. “Demonstration of Atomic Frequency Comb Memory for Light with Spin-Wave Storage”. *Phys. Rev. Lett.* **104**, 040503 (2010).
- [109] M. Businger, L. Nicolas, T. Sanchez Mejia, A. Ferrier, P. Goldner, and Mikael Afzelius. “Non-classical correlations over 1250 modes between telecom photons and 979-nm photons stored in $^{171}\text{Yb}^{3+}:\text{Y}_2\text{SiO}_5$ ”. *Nat Commun* **13**, 6438 (2022).
- [110] Shi-Hai Wei, Bo Jing, Xue-Ying Zhang, Jin-Yu Liao, Hao Li, Li-Xing You, Zhen Wang, You Wang, Guang-Wei Deng, Hai-Zhi Song, Daniel Oblak, Guang-Can Guo, and Qiang Zhou. “Quantum storage of 1650 modes of single photons at telecom wavelength” (2023). [arxiv:2209.00802](https://arxiv.org/abs/2209.00802).
- [111] Zong-Quan Zhou, Yi-Lin Hua, Xiao Liu, Geng Chen, Jin-Shi Xu, Yong-Jian Han, Chuan-Feng Li, and Guang-Can Guo. “Quantum Storage of Three-Dimensional Orbital-Angular-Momentum Entanglement in a Crystal”. *Phys. Rev. Lett.* **115**, 070502 (2015).
- [112] Antonio Ortu, Adrian Holzäpfel, Jean Etesse, and Mikael Afzelius. “Storage of photonic time-bin qubits for up to 20 ms in a rare-earth doped crystal”. *npj Quantum Inf* **8**, 1–7 (2022).
- [113] P. Jobez, I. Usmani, N. Timoney, C. Laplane, N. Gisin, and M. Afzelius. “Cavity-enhanced storage in an optical spin-wave memory”. *New J. Phys.* **16**, 083005 (2014).
- [114] Mahmood Sabooni, Qian Li, Stefan Kröll, and Lars Rippe. “Efficient Quantum Memory Using a Weakly Absorbing Sample”. *Phys. Rev. Lett.* **110**, 133604 (2013).
- [115] Jacob H. Davidson, Pascal Lefebvre, Jun Zhang, Daniel Oblak, and Wolfgang Tittel. “Improved light-matter interaction for storage of quantum states of light in a thulium-doped crystal cavity”. *Phys. Rev. A* **101**, 042333 (2020).
- [116] Ioana Craiciu, Mi Lei, Jake Rochman, Jonathan M. Kindem, John G. Bartholomew, Evan Miyazono, Tian Zhong, Neil Sinclair, and Andrei Faraon. “Nanophotonic Quantum Storage at Telecommunication Wavelength”. *Phys. Rev. Appl.* **12**, 024062 (2019).
- [117] Tian Zhong, Jonathan M. Kindem, John G. Bartholomew, Jake Rochman, Ioana Craiciu, Evan Miyazono, Marco Bettinelli, Enrico Cavalli, Varun Verma, Sae Woo Nam, Francesco Marsili, Matthew D. Shaw, Andrew D. Beyer, and Andrei Faraon. “Nanophotonic rare-earth quantum memory with optically controlled retrieval”. *Science* **357**, 1392–1395 (2017).
- [118] Morgan P. Hedges, Jevon J. Longdell, Yongmin Li, and Matthew J. Sellars. “Efficient quantum memory for light”. *Nature* **465**, 1052–1056 (2010).
- [119] J. J. Longdell, E. Fraval, M. J. Sellars, and N. B. Manson. “Stopped Light with Storage Times Greater than One Second Using Electromagnetically Induced Transparency in a Solid”. *Phys. Rev. Lett.* **95**, 063601 (2005).
- [120] J. Nunn, I. A. Walmsley, M. G. Raymer, K. Surmacz, F. C. Waldermann, Z. Wang, and D. Jaksch. “Mapping broadband single-photon wave packets into an atomic memory”. *Phys. Rev. A* **75**, 011401 (2007).
- [121] Pierre Jobez, Cyril Laplane, Nuala Timoney, Nicolas Gisin, Alban Ferrier, Philippe

- Goldner, and Mikael Afzelius. “Coherent Spin Control at the Quantum Level in an Ensemble-Based Optical Memory”. *Phys. Rev. Lett.* **114**, 230502 (2015).
- [122] Mustafa Gündoğan, Patrick M. Ledingham, Kutlu Kutluer, Margherita Mazzera, and Hugues de Riedmatten. “Solid State Spin-Wave Quantum Memory for Time-Bin Qubits”. *Phys. Rev. Lett.* **114**, 230501 (2015).
- [123] Shun Kanai, F. Joseph Heremans, Hosung Seo, Gary Wolfowicz, Christopher P. Anderson, Sean E. Sullivan, Mykyta Onizhuk, Giulia Galli, David D. Awschalom, and Hideo Ohno. “Generalized scaling of spin qubit coherence in over 12,000 host materials”. *Proceedings of the National Academy of Sciences* **119**, e2121808119 (2022).
- [124] Paul Stevenson, Christopher M. Phenicie, Isaiah Gray, Sebastian P. Horvath, Sacha Welinski, Austin M. Ferrenti, Alban Ferrier, Philippe Goldner, Sujit Das, Ramamoorthy Ramesh, Robert J. Cava, Nathalie P. de Leon, and Jeff D. Thompson. “Erbium-implanted materials for quantum communication applications”. *Phys. Rev. B* **105**, 224106 (2022).
- [125] Austin M. Ferrenti, Nathalie P. de Leon, Jeff D. Thompson, and Robert J. Cava. “Identifying candidate hosts for quantum defects via data mining”. *npj Comput Mater* **6**, 1–6 (2020).
- [126] Christopher M. Phenicie, Paul Stevenson, Sacha Welinski, Brendon C. Rose, Abraham T. Asfaw, Robert J. Cava, Stephen A. Lyon, Nathalie P. de Leon, and Jeff D. Thompson. “Narrow Optical Line Widths in Erbium Implanted in TiO₂”. *Nano Lett.* **19**, 8928–8933 (2019).
- [127] Mohammed K. Alqedra, Chetan Deshmukh, Shuping Liu, Diana Serrano, Sebastian P. Horvath, Safi Rafie-Zinedine, Abdullah Abdelatif, Lars Rippe, Stefan Kröll, Bernardo Casabone, Alban Ferrier, Alexandre Tallaire, Philippe Goldner, Hugues de Riedmatten, and Andreas Walther. “Optical coherence properties of Kramers’ rare-earth ions at the nanoscale for quantum applications” (2023). [arxiv:2303.02054](https://arxiv.org/abs/2303.02054).
- [128] Diana Serrano, Senthil Kumar Kuppusamy, Benoît Heinrich, Olaf Fuhr, David Hunger, Mario Ruben, and Philippe Goldner. “Ultra-narrow optical linewidths in rare-earth molecular crystals”. *Nature* **603**, 241–246 (2022).
- [129] Tian Zhong and Philippe Goldner. “Emerging rare-earth doped material platforms for quantum nanophotonics”. *Nanophotonics* **8**, 2003–2015 (2019).
- [130] Mikael Afzelius and Christoph Simon. “Impedance-matched cavity quantum memory”. *Phys. Rev. A* **82**, 022310 (2010).
- [131] Manish Kumar Singh, Liang Jiang, David D. Awschalom, and Supratik Guha. “Key Device and Materials Specifications for a Repeater Enabled Quantum Internet”. *IEEE Transactions on Quantum Engineering* **2**, 4102909 (2021).
- [132] M. Pompili, S. L. N. Hermans, S. Baier, H. K. C. Beukers, P. C. Humphreys, R. N. Schouten, R. F. L. Vermeulen, M. J. Tiggeleman, L. dos Santos Martins, B. Dirkse, S. Wehner, and R. Hanson. “Realization of a multinode quantum network of remote solid-state qubits”. *Science* **372**, 259–264 (2021).
- [133] W. J. Munro, K. A. Harrison, A. M. Stephens, S. J. Devitt, and Kae Nemoto. “From quantum multiplexing to high-performance quantum networking”. *Nature Photon* **4**, 792–796 (2010).
- [134] F. Kimiaee Asadi, S. C. Wein, and C. Simon. “Protocols for long-distance quantum communication with single ¹⁶⁷Er ions”. *Quantum Sci. Technol.* **5**, 045015 (2020).
- [135] F. Kimiaee Asadi, N. Lauk, S. Wein, N. Sinclair, C. O’Brien, and C. Simon. “Quantum repeaters with individual rare-earth ions at telecommunication wavelengths”. *Quantum* **2**, 93 (2018).

- [136] Mouktik Raha, Songtao Chen, Christopher M. Phenicie, Salim Ourari, Alan M. Dibos, and Jeff D. Thompson. “Optical quantum nondemolition measurement of a single rare earth ion qubit”. *Nat Commun* **11**, 1605 (2020).
- [137] Songtao Chen, Mouktik Raha, Christopher M. Phenicie, Salim Ourari, and Jeff D. Thompson. “Parallel single-shot measurement and coherent control of solid-state spins below the diffraction limit”. *Science* **370**, 592–595 (2020).
- [138] Alexander Ulanowski, Benjamin Merkel, and Andreas Reiserer. “Spectral multiplexing of telecom emitters with stable transition frequency”. *Science Advances* **8**, eabo4538 (2022).
- [139] David Awschalom, Karl K. Berggren, Hannes Bernien, Sunil Bhave, Lincoln D. Carr, Paul Davids, Sophia E. Economou, Dirk Englund, Andrei Faraon, Martin Fejer, Saikat Guha, Martin V. Gustafsson, Evelyn Hu, Liang Jiang, Jungsang Kim, Boris Korzh, Prem Kumar, Paul G. Kwiat, Marko Lončar, Mikhail D. Lukin, David A.B. Miller, Christopher Monroe, Sae Woo Nam, Prineha Narang, Jason S. Orcutt, Michael G. Raymer, Amir H. Safavi-Naeini, Maria Spiropulu, Kartik Srinivasan, Shuo Sun, Jelena Vučković, Edo Waks, Ronald Walsworth, Andrew M. Weiner, and Zheshen Zhang. “Development of Quantum Interconnects (QuICs) for Next-Generation Information Technologies”. *PRX Quantum* **2**, 017002 (2021).
- [140] Nikolai Lauk, Neil Sinclair, Shabir Barzanjeh, Jacob P. Covey, Mark Saffman, Maria Spiropulu, and Christoph Simon. “Perspectives on quantum transduction”. *Quantum Sci. Technol.* **5**, 020501 (2020).
- [141] Morten Kjaergaard, Mollie E. Schwartz, Jochen Braumüller, Philip Krantz, Joel I.-Jan Wang, Simon Gustavsson, and William D. Oliver. “Superconducting Qubits: Current State of Play”. *Annu. Rev. Condens. Matter Phys.* **11**, 369–395 (2020). [arxiv:1905.13641](#).
- [142] Maud Vinet. “The path to scalable quantum computing with silicon spin qubits”. *Nat. Nanotechnol.* **16**, 1296–1298 (2021).
- [143] Lewis A. Williamson, Yu-Hui Chen, and Jevon J. Longdell. “Magneto-Optic Modulator with Unit Quantum Efficiency”. *Phys. Rev. Lett.* **113**, 203601 (2014).
- [144] Faezeh Kimiaee Asadi, Jia-Wei Ji, and Christoph Simon. “Proposal for transduction between microwave and optical photons using ^{167}Er -doped yttrium orthosilicate”. *Phys. Rev. A* **105**, 062608 (2022).
- [145] Jake Rochman, Tian Xie, John G. Bartholomew, K. C. Schwab, and Andrei Faraon. “Microwave-to-optical transduction with erbium ions coupled to planar photonic and superconducting resonators”. *Nat Commun* **14**, 1153 (2023).
- [146] John G. Bartholomew, Jake Rochman, Tian Xie, Jonathan M. Kindem, Andrei Ruskuc, Ioana Craiciu, Mi Lei, and Andrei Faraon. “On-chip coherent microwave-to-optical transduction mediated by ytterbium in YVO_4 ”. *Nature Communications* **11**, 3266 (2020).
- [147] Xavier Fernandez-Gonzalvo, Sebastian P. Horvath, Yu-Hui Chen, and Jevon J. Longdell. “Cavity-enhanced Raman heterodyne spectroscopy in $\text{Er}^{3+}:\text{Y}_2\text{SiO}_5$ for microwave to optical signal conversion”. *Phys. Rev. A* **100**, 033807 (2019).
- [148] Sacha Welinski, Philip J. T. Woodburn, Nikolai Lauk, Rufus L. Cone, Christoph Simon, Philippe Goldner, and Charles W. Thiel. “Electron Spin Coherence in Optically Excited States of Rare-Earth Ions for Microwave to Optical Quantum Transducers”. *Phys. Rev. Lett.* **122**, 247401 (2019).